

**United States
Department of
Agriculture**



**Agricultural
Research Service**

**Southern Plains Area
Cropping Systems Research
Laboratory**

**Wind Erosion and Water
Conservation Research**

Technical Bulletin No. 2
February 15, 1999

**El Niño and La Niña Related
Climate and Agricultural Impacts
over the
Continental United States**

by
Steven A. Mauget and Dan R. Upchurch

Table of Contents

I.	INTRODUCTION	3
II.	METHODS AND DATA	5
III.	EL NIÑO CLIMATE IMPACTS	7
	a) El Niño Summer (JJA-JAS-ASO)	7
	b) El Niño Fall-Winter (SON-OND-NDJ-DJF)	7
	c) El Niño Winter-Spring (JFM-FMA-MAM-AMJ)	8
IV.	LA NIÑA CLIMATE IMPACTS	8
	a) La Niña Summer (JJA-JAS-ASO)	8
	b) La Niña Fall-Winter (SON-OND-NDJ-DJF).....	9
	c) La Niña Winter-Spring (JFM-FMA-MAM-AMJ)	9
V.	ENSO EFFECTS ON CORN AND WINTER WHEAT YIELDS	9
	a) Corn Yield Effects	11
	b) The “post-El Niño phenomenon”	13
	c) Winter Wheat Yield Effects	15
VI.	DISCUSSION	15
	a) Summer Climate and Yield Impacts	15
	b) Winter Climate and Yield Impacts	18
	c) ENSO and the Potential for Seasonal Forecasts of Opportunity	19
	d) ENSO Forecasts of Opportunity and Agricultural Management	19
VII.	CONCLUSION	20
	WORLD WIDE WEB RESOURCES	23
	REFERENCES	24
	APPENDIX A	27
	APPENDIX B	39
	APPENDIX C	51

I. INTRODUCTION

The uncertainty of climate makes the year-to-year practice of farming similar to an ongoing game of chance. Every year before planting the farmer decides what and how much to grow (or, if to grow) and then gambles on whether climate conditions during the growing season will allow his management decisions to, in effect, “pay off”. Predicting seasonal growing conditions before planting could have the effect of improving the odds in the farmer’s favor. However, seasonal climate prediction requires climate mechanisms that actually behave predictably over season-to-season time scales. As a result, the potential for forecasting seasonal climate might be gauged by considering the following two necessary conditions: 1) that deterministic mechanisms exist in the Earth’s climate system that are capable of shifting a region’s seasonal climate from its long term mean, and, 2) that those mechanisms persist or evolve predictably over inter-seasonal (i.e., season-to-season) time scales. One mechanism that has demonstrated both the ability to produce shifts in seasonal climate over the continental United States and the potential for inter-seasonal predictability is the El Niño–Southern Oscillation (ENSO).

The effects of the ENSO mechanism on agriculture played an important role in motivating early research. The critical dependence of Indian food production on monsoonal rainfall and the failure of the Indian monsoon in 1877 inspired early forecasting attempts by the India Meteorological Department (Allan et al. 1996). Related research involved efforts to summarize large scale atmospheric conditions associated with the Indian monsoon, which lead to the identification of a near-global scale oscillation in surface pressure over the Indian and Pacific Oceans that Sir Gilbert Walker¹ referred to as the Southern Oscillation. The term El Niño has been in use along the Peruvian coast since at least 1895 (Philander 1990) and refers to a southward moving counter-current of warm water appearing around Christmas of each year which fishermen dubbed El Niño (“the boy child”) in honor of Christ. Year-to-year variability in the state of the Southern Oscillation and in the strength and persistence of the El Niño current were considered as occurring independently until the 1960’s, when Bjerknes (1969) proposed a dynamic synthesis linking the large scale variation in atmospheric surface pressure and eastern Pacific sea-surface temperature. The current conception of ENSO (Philander 1990; Trenberth 1991; Allan et al. 1996) is that of a coupled ocean-atmosphere phenomenon primarily active over the tropics and subtropics of the Pacific and Indian Oceans. The connection between atmospheric and oceanic components are expressed in a mutual interplay between the organization of large scale vertical circulations in the atmosphere and the warm and cold sea-surface temperature anomalies (SSTA) that both drive and are driven by these circulations. The state of ENSO is measurable through anomalies in surface pressure and sea-surface temperature which vary in amplitude and sign over inter-annual time scales, and the related oscillatory nature of the underlying mechanism has led to its description in terms of two distinct phases. The La Niña phase is marked by the upwelling of cold sub-surface water along the equator in the eastern Pacific and the western coast of South America, thus the alternate designation of cold phase conditions. Conversely, the coupled ocean-atmosphere dynamics associated with the El Niño phase produce anomalously warm sea-surface temperatures in the central and eastern equatorial Pacific, thus the designation warm phase. Both phases produce anomalous atmospheric circulation conditions over the North Pacific and North America (Bjerknes 1969; Trenberth and Shea 1987; Barnston et al. 1991; Hoerling et al. 1997) which can significantly affect North American climate (Ropelewski & Halpert 1986, 1989; Bunkers et al. 1996; Montroy 1997; Livezey et al. 1997) over seasonal time scales.

¹ Director-General of Observatories in India 1904-1924. 3

The sign and magnitude of equatorial Pacific sea-surface temperature anomalies provide a measure of ENSO phase and strength. In addition, the relative frequency with which monthly SSTA assumes extreme values reveals a tendency for the mechanism to be active during certain parts of the seasonal cycle. Figure 1a shows the number of calendar months over the period 1895-1997 during which SSTA anomalies in the eastern equatorial Pacific were in the highest (warmest) 17% and 10% of the 1895-1997 distribution. Although instances of anomalous warm temperatures are evident during the spring and summer months, the broad peak spanning September-February shows that the El Niño phase is mainly active during the northern fall and winter months. The tendency for highest decile conditions to occur during November-December-January indicates that the strength of events tends to peak during that period. Rasmusson and Carpenter (1982) outline a composite of the evolution of El Niño events and identify this approximate seasonal time window with the mature phase of El Niño development. These periods are associated with the highest magnitudes of positive sea-surface temperature anomalies in the equatorial Pacific, and the strongest impact on Northern Hemisphere atmospheric circulation. Figure 1b is the cold phase counterpart to Fig. 1a; i.e., the distribution of calendar months over the period 1895-1997 during which eastern Pacific SSTA was in the lowest (coldest) 17% and 10%. A tendency for La Niña conditions to occur during a well defined northern winter period is not as evident, with both November and February suggested as periods of peak activity. However, given an apparent overall tendency for cold phase SST conditions to occur in the northern winter months, the notion of mature La Niña conditions during such periods may also be useful as a seasonal marker of peak development. As a result, a simple time line consisting of pre-mature, mature, and post-mature periods will be used here to describe the development of both phases.

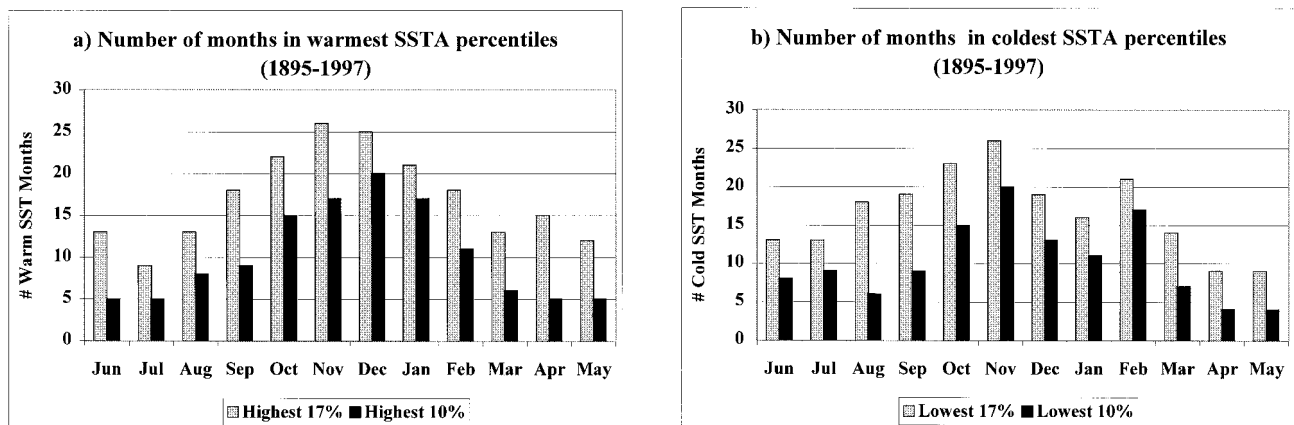


Fig. 1. a) Gray(Black) bars indicate the number of calendar months over the period 1895-1997 during which Wright's (1989) eastern Pacific SSTA ('S') index was in the warmest 17% (10%) of the 1895-1997 distribution. b) As in (a) for number of calendar months during which the S index was in the coldest 17% (10%) of the 1895-1997 distribution.

The goal of this technical report is to supplement information found in Mauget and Upchurch (1999). That research explored the relationship between the state of ENSO-related SST anomalies over the equatorial eastern Pacific and concurrent shifts in seasonal climate over the central United States, and also evaluated associated agricultural effects. This report expands the climate analysis to the entire continental United States, and presents results relevant to a broader range of seasonal time windows. Part II outlines the methods and data used here to seek out significant SST-climate relationships. Part III describes the effects on seasonal

temperature and precipitation associated with the El Niño phase, while part IV describes the effects associated with the La Niña phase. Part V presents an analysis of the effects of both ENSO phases on corn and winter wheat yields. Part VI discusses both summer and winter climate and yield effects, the prospects for seasonal forecasts of opportunity during active ENSO periods, and how those forecasts might affect agricultural management. The conclusion proposes, based on a gambling-agriculture analogy, that the potential for long-term economic gain derived from ENSO forecasts of opportunity may be greater for winter wheat producers than for corn producers.

II. METHODS AND DATA

The climate analysis method used here compares the distribution of seasonal climate values sampled during periods consistent with El Niño and La Niña SST conditions with the sampling probabilities associated with a null hypothesis that assumes random sampling from the historical climate record. Significant ENSO-related skewness in seasonal climate may be evident in a sample of seasonal data values when that sample's incidence of values above or below the median of the population from which it is drawn, or in the extreme percentiles of that population, is inconsistent with random sampling at a specified confidence level.

Wright's (1989) S index (S) is used here to identify seasonal periods consistent with both ENSO phases. The S index provides a continuous historical record (1881-1986) of SST anomalies averaged over an irregular region of the equatorial Pacific (see Fig.2) extending from the dateline to 90W and 6N to 10 S. The S index was extended here by regressing it against Niño 3.4 SSTA values during the 1950-1986 period, and using the resulting regression coefficients and Niño 3.4 values during 1987-1997 to infer S values over that 11 year period.

The state of seasonal climate over the continental U.S. was determined through the use of U.S. Climate Division Data (Guttman and Quayle 1996). Climate Division precipitation (temperature) data is reported as monthly totals (averages) over each of the continental United State's 344 climate divisions. The data used here extends over the 103 year period between January 1895 and December 1997. Before analysis, each climate division's monthly rainfall (temperature) data was converted to seasonal values by summing (averaging) the monthly data values over consecutive and overlapping three month periods (January-February-March = JFM, February-March-April = FMA, ... December-January-February = DJF, etc.). These values were then ranked from the smallest seasonal value over the 103 year period of record (Jan. 1895–Dec. 1997) to the largest. The resulting order statistics were then used to determine thresholds marking the lowest 25% of values (i.e., the lowest quartile), the highest 25% of values (i.e., the highest quartile) and the 50th percentile (i.e., the median) in the manner suggested by Wilks (1995). This process was repeated for each climate division over each three month seasonal time window.

ENSO seasons were identified as those three month periods during which the average S index value exceeded extreme threshold values. The S index is not normally distributed, thus thresholds marking the lowest and highest 17 % and 10% of historical S values were used here as robust approximations of the first and second standard deviations of the S index distribution. Seasons of moderate and strong El Niño conditions were defined as those three month periods during which the average S index value was in the highest 17% ($> +0.84$ C) of the 1895-1997 distribution of S values. Conversely, three month periods during which the average S value was in the lowest 17% (< -0.64 C) marked seasons of moderate and strong La Niña conditions. Periods of strong El Niño forcing were identified as those seasons during which the average S

Wright's S Index (1895-1997)

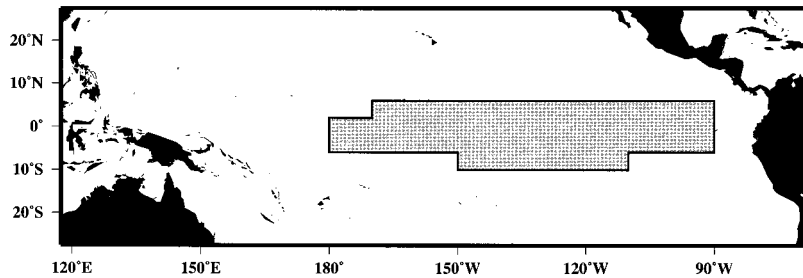
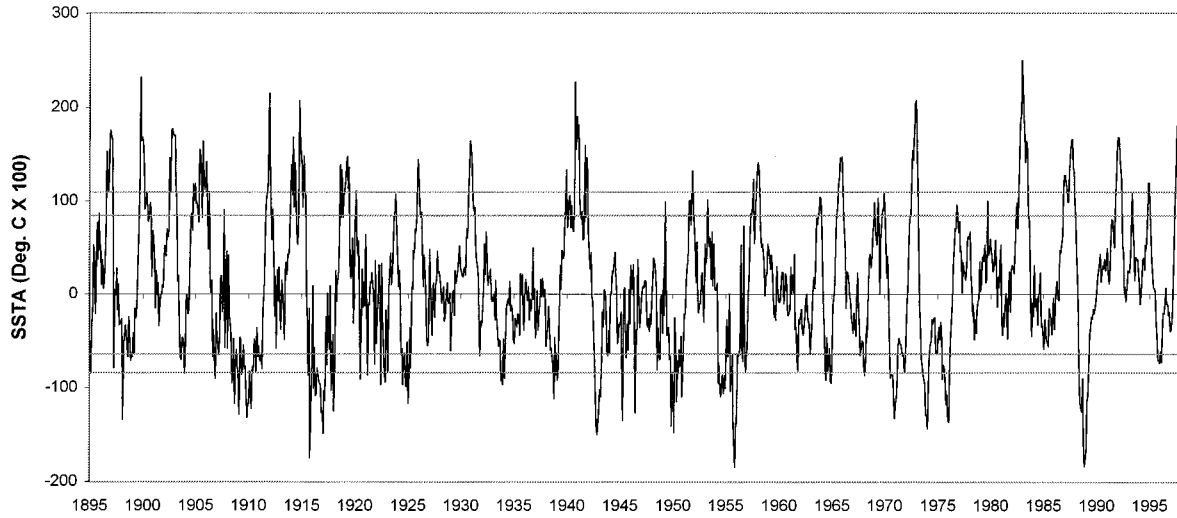


Fig. 2 (Top) Time series of Wright's (1989) eastern Pacific SSTA index. Values after 1987 were regressed from Niño 3.4 SSTA values. Horizontal gray lines indicate highest (+0.84 C) and lowest (-0.64 C) sextile values, and highest (+1.09 C) and lowest (-0.84 C) decile values. (Bottom) Wright's (1989) eastern equatorial Pacific averaging region.

value was in the highest 10% of historical values, ($> +1.09^{\circ} \text{C}$), while strong La Niña conditions were defined by S values in the lowest 10% ($< -0.84^{\circ} \text{C}$). For notational purposes these percentiles will at times be indicated by 10-, 10+, 17-, and 17+, with 10+ (10-) indicating the highest (lowest) 10%, etc.

The climate tests found in Appendix A were conducted on samples of climate division data consistent with periods of moderate and strong (17+) El Niño conditions, while Appendix B contains tests consistent with moderate and strong La Niña (17-) conditions. The climate tests found in Appendix C were conducted on samples of climate division data consistent with summer periods marked by strong (10-) La Niña conditions. In those figures climate divisions are shaded or hatched where it was found that the seasonal rainfall or temperature during the indicated seasons was significantly skewed about the division's 1895-1997 seasonal median value. If results indicated a significant incidence of extreme seasonal rainfall or mean temperature, defined here as the lowest and highest 25% of the historical record. Annotated climate divisions indicate those that showed a significant incidence of extreme climate conditions. Climate divisions that are both shaded and annotated allow offer a more complete breakdown of how seasonal climate during anomalous ENSO conditions fell within the historical distribution. For example, in the July-August-

September (JAS) rainfall analysis of Appendix A (Fig. A2) the shading of Nebraska's westernmost climate division shows that of the 13 seasons indicated, 12 were above the 103 year median for July-August-September rainfall. The annotation (0/6) shows that none of those 13 seasons resulted in rainfall in the first (driest) 25% of the historical record, while 6 seasons resulted in rainfall in the highest (wettest) 25%. Twelve seasons were above the median while 6 were in the highest 25%, thus 6 JAS periods fell in the 50th – 75th percentile. As 1 season was below the median but not in the lowest 25%, that season fell in the 25th – 50th percentile. As a result, those 13 El Niño seasons resulted in 0-1-6-6 instances occurring in the 1st-2nd-3rd-4th 25% of that climate division's historical distribution of JAS seasonal rainfall values. Although the sequence of seasonal skewness analyses found in Appendices A-C may appear to show evolving climate impacts, they should not be interpreted as reflecting the evolution of a composite ENSO event. Instead, they should be considered simply as statistical analyses of seasonal climate, conditional on the concurrent state of SST in the equatorial Pacific.

III. EL NIÑO CLIMATE IMPACTS

a) El Niño Summer (JJA-JAS-ASO)

Of the three warm phase summer season analyses found in Appendix A, the July-August-September time window shows the most widespread evidence of skewed seasonal climate. Figure A2 shows the analyses for rainfall and temperature during JAS seasons marked by S index conditions in the highest 17%. Of those 13 seasons, all but two (1900 and 1987) are consistent with pre-mature phase summer periods. The predominant climate effects are that of cool and wet conditions over parts of the central and western United States.

- ◆ Over major portions of the Missouri River drainage region a significant tendency to above median rainfall and below median temperature is evident. A tendency to seasonal temperatures below the median and in the lowest 25% is evident over parts of the Great Plains and over climate divisions straddling the Rocky Mountain region. From an agricultural perspective, evidence of extreme (i.e., highest 25%) seasonal rainfall in corn belt climate divisions in eastern Nebraska, Iowa, and northern Illinois is particularly interesting.
- ◆ In climate divisions in Michigan and Wisconsin a tendency to cool summer conditions is evident.
- ◆ A significant incidence of seasonal precipitation below the median and in the lowest 25% is found within a cluster of climate divisions extending from West Virginia to New Jersey.

b) El Niño Fall-Winter (SON-OND-NDJ-DJF)

During fall and early winter periods (Figs. A4-A7) marked by warm SST conditions in the eastern equatorial Pacific a number of significant climate effects become apparent over the continental United States.

- ◆ In the southwestern, southern, and central U.S a significantly increased incidence seasonal precipitation above the median and in the highest 25% is evident. In the SON analysis (Fig. A4) this tendency towards wetter seasonal conditions is apparent over the Southwest, Texas, and parts of the Central Great Plains. One rainfall effect found in the SON analysis but not in the ASO or OND precipitation analyses is a highly significant tendency to increased rainfall over Nevada and Southern California. In the OND precipitation analysis this region shows no significant rainfall effect, but evidence of in-

creased rainfall over Florida does become apparent. In the DJF precipitation analysis (Fig. A7) a significant incidence of precipitation above the median and in the highest 25% is found over major winter wheat growing regions of Texas, Oklahoma, Kansas, and Nebraska.

- ◆ In the NDJ (Fig. A6) and DJF (Fig. A7) precipitation analyses a significant shift to below median precipitation is evident over the Northern Great Plains and the Dakotas.
- ◆ In the NDJ and DJF temperature analyses, significant and widespread tendencies to seasonal temperatures above the median and in the highest 25% are found over the northernmost tier of states. Conversely, a significant incidence of below median seasonal temperatures is found over climate divisions along and adjacent to the coast of the Gulf of Mexico.

c) El Niño Winter-Spring (JFM-FMA-MAM-AMJ)

Climate effects during warm phase winter and spring periods (Figs. A8-A11) are qualitatively similar to that found in the Fall-Winter seasonal time windows, with some variation in the extent and distribution of those impacts.

- ◆ As in the DJF precipitation analysis, the JFM (Fig. A8) and FMA (Fig. A9) analyses show a tendency to precipitation above the median and above the highest quartile over the Southwest and along the Gulf Coast and Florida, and over the winter wheat growing regions of the central U.S. In the MAM and AMJ precipitation analyses (Figs. A10 & 11) this tendency to seasonal wetness is restricted to climate divisions in Texas and the Southwest.
- ◆ The JFM and FMA precipitation analyses show evidence of a significant incidence of below median precipitation over Montana, with no such indications in the MAM analysis. Evidence of significant dryness over the Ohio River Valley – first apparent in the DJF precipitation analysis – can be found in the increased incidence of extreme seasonal dryness over that region during JFM and FMA.
- ◆ The tendency to warmer conditions found over the northernmost tier of states in the DJF temperature analysis appears shifted to the west in the JFM, FMA, MAM, and AMJ analyses. The incidence of cool seasonal conditions over the southern and southeastern U.S. is much more extensive in the temperature analyses of Figs. A8-A10, with the greatest extent of conditions below the median and in the lowest 25% found during FMA.

IV. LA NIÑA CLIMATE IMPACTS

a) La Niña Summer (JJA-JAS-ASO)

The skewness analyses of La Niña summer periods marked by S index conditions in the lowest 17% (Figs. B1-B3) reveal only scattered indications of significant climate effects. However, when seasonal climate conditions concurrent with strong La Niña summer conditions (i.e., SST anomalies in the lowest 10% of historical S index values, see Figs. C1-C3) are tested for skewness, significant and consistent seasonal temperature effects become apparent.

- ◆ Over corn belt climate divisions during JJA and JAS, Figures C1 and C2 show a significant incidence of seasonal temperatures above the median and above the highest quartile during periods marked by extreme cold (“10-“ equatorial Pacific SST conditions. The shaded Iowa and Illinois climate divisions

annotated 0/3 in Fig. C1 show that those seasons resulted in 0-0-1-3 instances occurring in the 1st-2nd-3rd-4th 25% of JJA temperature. In Fig. C2 the shaded Illinois climate divisions annotated 1/4 show that those seasons resulted in 1-0-2-4 instances occurring in the 1st-2nd-3rd-4th 25% of JAS temperature.

b) La Niña Fall-Winter (SON-OND-NDJ-DJF)

During fall and winter periods (Figs. B4-B7) marked by “17-“ S index conditions the most significant climate effects over the U.S. are that of dryness and warmth over lower latitude regions, cold conditions over the Northern Plains, and increased precipitation in the northwest.

- ◆ In Fig. B4 a consistent tendency to below median SON precipitation is evident from Southern California to Arkansas. In the OND (Fig. B5) analysis tendencies to seasonal precipitation in the lowest 25% are more evident over this broad region, with scattered indications of dryness extending northward into the Midwest. In the NDJ and DJF analyses (Figs. B6 and B7) the tendency to extremely dry winter conditions becomes evident in the southeastern states.
- ◆ In the SON temperature analysis of Fig. B4 a uniform tendency to above median temperatures is evident over the Midwest, with scattered evidence of seasonal temperatures in the highest 25%. In the OND and NDJ analyses a highly uniform tendency to seasonal temperatures in the highest 25% of the historical record. is evident over the south-central U.S.

c) La Niña Winter-Spring (JFM-FMA-MAM-AMJ)

The most notable climate effects evident during cold phase winter and spring periods (Figs. B8-B11) are dry and warm conditions found in earlier seasonal time windows throughout the southern, central, and southeastern U.S..

- ◆ In Fig. B8 a tendency to JFM precipitation below the median and in the lowest 25% is apparent over the Carolinas, Florida and the Gulf Coast. A higher incidence of dry seasonal conditions is also indicated over winter wheat producing regions in Texas, Oklahoma, Kansas, and Nebraska, which is also apparent in the analysis of FMA precipitation (Fig. B9). Figure B9 also shows a significant tendency to dry conditions over Southern California and the desert southwest.
- ◆ The analysis of JFM temperature shows a consistent tendency to seasonal temperatures in the highest 25% of historical values over the southern and southeastern U.S., and the Ohio River Valley.

V. ENSO EFFECTS ON CORN AND WINTER WHEAT YIELDS

There are a number of seasonal precipitation and temperature effects apparent in Appendices A-C that could potentially impact agriculture over the continental United States. However, given the tendency to significant shifts in climate over corn and winter wheat producing regions during El Niño and La Niña conditions, and the desire to compare effects on both a winter and summer crop, the emphasis here will be on those two crops.

The historical records of per-acre yield of both corn and winter wheat (Fig. 3a) show monotonic increasing trends beginning in the middle decades of the 20th century. Mjelde and Keplinger (1998) discuss numerous reasons for the increase in wheat productivity in the years following World War II, while Handler (1984) cites the introduction of hybrid corn and the use of nitrogen fertilizers as factors contributing to higher

corn yields. Determining significant inter-annual fluctuations in yield about these long term trends requires a year-to-year estimate of the trend values themselves. To solve for long-term trends in per-acre yields, USDA-NASS historical statewide yield estimates were first subjected here to a 71 point low-pass Lanczos filter (Duchon 1979). Using such a selective low pass filter and a cutoff period of 25 years, the resulting long term trends are essentially the yield records minus all spectral components with a period of less than 25 years. Using the yield (y) and resulting trend values (t) for a particular year, Percentage Departure from Trend (PDT) values are given by

$$\text{PDT} = \frac{y - t}{t} \quad .$$

“Normal” yields for a specified year are approximated by the year’s trend value, thus the PDT values estimate a year’s percentage departure from normal. Near normal yields were defined as the 1/3 of all yield values closest to the long-term trend line. Threshold values separating above from near, and near from below normal yield values were estimated by determining constants bounding the ~ 1/3 of values in a PDT time series closest to 0.0. As a result, the total number of harvests were divided into above, near, and below normal classes of approximately equal number. The PDT constants separating these classes varied in magnitude from .06 to .09, depending upon each state’s yield record. For a threshold value of .06 near normal yield for a given year was defined as being within +/- 6% of the year’s long-term trend value, while above(below) normal yields were defined as those greater than(less than) 106%(94%) of trend. The magnitudes of these thresholds can be compared with the value of .03 used by Handler (1984, 1990) and .10 used by Carlson et al. (1996).

As in the analysis of historical climate data, hypergeometric null distributions were used to check whether the incidence of above and below normal yields in post-warm and post-cold phase harvests were significantly different from that expected from random sampling (Eq. 1, Fig. 3c). When yields were tested for a significant incidence of above normal values, near and below normal yields were grouped into one class. To test for a significant incidence of below normal yields, near and above normal yields were grouped together, etc. Table 1 shows the results for the corn yield analyses, while Table 3 shows the results for winter wheat. Thus, for example, Table 1 (also, see Fig. 4) shows that of 12 post-El Niño Illinois corn harvests, none resulted in below normal per-acre yields, while 3 were near normal and 9 were above normal. Selecting 12 harvests from a 114 year record consisting of 31 below, 37 near, and 46 above normal yields and sampling 9 above normal is significant at a 98.8% confidence level. As a result, a significant tendency for above normal yields is evident, conditional on “17+” JAS S index values. Figure 4 graphs the percentage departure from trend (PDT) values for corn after the warm and cold SST summer periods of Table 1, and the PDT values for wheat yields after the warm and cold phase winter periods of Table 3. That figure is intended to compare significant departures in post-ENSO corn and winter wheat yields after summer and winter periods marked by SSTA conditions in the lowest and highest 17% of the historical record. Departures significant at a 90% confidence level or better are shaded in gray, and the annotation adjacent to that shading shows the actual significance level.

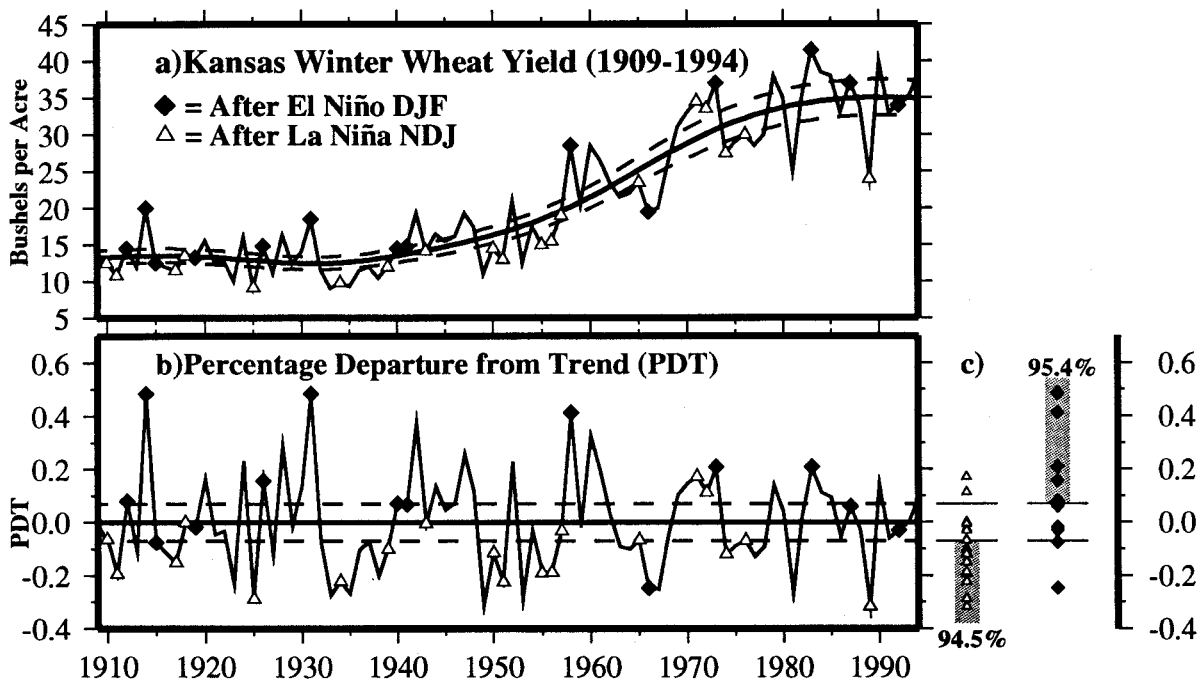


Fig. 3. a) USDA-NASS per acre historical yields for Kansas winter wheat and long term trend line. Dashed curves delimit above, near and below normal yield values. Diamond shaped data points indicate harvests after DJF periods exhibiting mean S index values in the highest 17%, while triangles mark harvests after NDJ periods marked by seasonal S values in the lowest 17%. b) Percentage Departure from Trend values [(yield-trend)/trend] for Kansas winter wheat. c) Distribution of below, near, and above normal yields in post-El Niño and post La Niña harvests, as determined by procedure described in text. Grey bars indicate sampling patterns significantly different from random sampling at a 90% confidence level or better, and bar annotation shows associated significance levels.

a) Corn Yield Effects

Of the summer season climate analyses found in Appendices A-C only the JAS season showed evidence of significant climate shifts during both warm and cold S index conditions. As a result, corn yields harvested in the fall seasons immediately after warm and cold SST JAS seasons were tested as described above. This yield analysis was conducted over a longer time period than that of the climate analysis, as NASS corn yield records extend back to 1866. However, as Wright's S index has numerous data gaps prior to 1881 only per acre yield values after the harvest of 1880 were used here. The post-warm phase yield values sampled from the 1881-1994 records were those harvested after the first 12 El Niño JAS periods of Fig. A2, as no JAS periods exhibiting S index values in the highest 17% were found during 1881-1895. Although significant climate effects during La Niña summers were only evident when S index conditions were in the lowest 10%, we sampled corn yields immediately after JAS periods during which SSTA conditions were in the lowest 17%. This was done given the desire to conduct both corn and winter wheat yield analyses based on comparable SSTA thresholds. The post-cold phase per-acre yields sampled correspond to harvests immediately after the 14 La Niña JAS seasons of Fig. B2, and after 4 other JAS seasons that saw S index conditions in the lowest 17% during 1881-1895.

As noted before, Illinois corn yields show a significant tendency for above normal values conditional on JAS S index values in the highest 17%. A significant (96.2 %) incidence of above normal Indiana yields after warm SST JAS periods is also shown in Table 1 and Fig. 4. A significant incidence of below normal yields after the 18 La Niña JAS periods is also found in both states, with a particularly high number of below

TABLE 1: Corn yields after ENSO summer seasons

State	Harvests #	Below Normal	Near Normal	Above Normal	Significance %
Colorado					
After Warm DJF (17+)	14	4	3	<u>7</u>	90.5
After Cold NDJ (17-)	20	<u>11</u>	4	5	92.9
All Years (1909-1994)	86	33	26	27	NA
Kansas					
After Warm DJF (17+)	14	2	4	<u>8</u>	95.4
After Cold NDJ (17-)	20	<u>11</u>	7	2	94.5
All Years (1909-1994)	86	32	25	29	NA
Nebraska					
After Warm DJF (17+)	14	4	3	<u>7</u>	88.5
After Cold NDJ (17-)	20	<u>11</u>	2	7	94.5
All Years (1909-1994)	86	32	26	28	NA
Oklahoma					
After Warm DJF (17+)	14	2	4	<u>8</u>	96.3
After Cold NDJ (17-)	20	<u>14</u>	3	3	99.9
All Years (1909-1994)	86	31	27	28	NA
Texas					
After Warm DJF (17+)	14	0	4	<u>10</u>	99.8
After Cold NDJ (17-)	20	<u>13</u>	5	2	99.5
All Years (1909-1994)	86	32	26	28	NA

Table 1. Entries show the number of total and below, near, and above normal corn harvests after July-August-September (JAS) periods marked by anomalously warm and cold SST conditions in the equatorial eastern Pacific. "All years" entries indicate those same counts for the (1881-1994) population of harvests for each state. 17+ and 17- indicate S index conditions in the highest 17% and lowest 17%, of the distribution of historical (1895-1997) values. Significance levels apply to the bold and underlined entries in each row. Thus underlined near and above normal counts shows a tendency for near and above normal harvests at the corresponding significance level, etc. yields after the 18 La Niña JAS periods is also found in both states, with a particularly high number of below normal yields (10) in Illinois. Thus corn yields in both states appear to be positively correlated with July-August-September SST anomalies in the equatorial Pacific.

normal yields (10) in Illinois. Thus corn yields in both states appear to be positively correlated with July-August-September SST anomalies in the equatorial Pacific.

A significant incidence of above normal yields is not evident in the 12 post-El Niño Iowa corn harvests, and a tendency for near or above normal Iowa yields after JAS periods marked by warm S index conditions is also not found here at a 90% confidence level. However, as the cumulative probability of randomly selecting 3 or less above normal yields in a sample of 18 from the Iowa population is 5.2%, there is a significantly reduced incidence of above normal Iowa yields after JAS periods marked by cold (“17-“) SST conditions. As a result, a significant (i.e., 94.8%) tendency for near or below normal Iowa yields after La Niña summer conditions is indicated. The distribution of Nebraska corn yields harvested after JAS periods marked by warm and cold S values resembles that of Iowa. Of 12 Nebraska harvests after El Niño JAS conditions 7 were above normal, which is significant at an 86.4% confidence level. This suggests a somewhat stronger tendency for above normal yields than in the Iowa record, though not significant at a 90% confidence level. The distribution of Nebraska yields after La Niña JAS conditions is identical to that of the Iowa, and like the Iowa results a significant tendency for near or below normal yields is found.

Of the 12 instances of Minnesota yields harvested after warm S index JAS periods, 9 were above normal, but the remaining three were below normal. Although sampling 9 above normal harvests in a sample of 12 from the Minnesota population is significant at a 98.3% confidence level, a significant decrease in below normal yields is not apparent. In harvests after summer periods marked by La Niña SSTA conditions, a tendency for near and below normal yields seems apparent, although not at a 90% confidence level.

b) The “post-El Niño phenomenon”

Garnett and Khandekar (1992) note that major U.S corn crop failures in 1980, 1983, and 1987 occurred immediately after the weak El Niño event of 1979/80 and the strong and moderate events of 1982/83 and 1986/87. These instances of mature warm phase conditions during the northern winter months followed by crop failure during the subsequent summer growing season have led some to suggest the existence of a “post-El Niño phenomenon” linking El Niño events to reduced corn yields. To check for the existence of such a lagged climate-yield relationship – the cause and effect aspects of which are not clear – the distribution of per-acre corn yields for the states considered above were tested for significant skewness in years following 17 mature El Niño periods². The criterion for selecting these 17 warm phase winter periods was that average October-February S index values exceed the 1895-1997 “17+” S index threshold. In the case of multiple year events such as those occurring over 1904-06 and 1939-41 only harvests after the last Oct.-Feb. mature period were considered, provided the period satisfied the S threshold criterion. The results of this analysis can be found in Table 2, and if any post-El Niño trend in corn yields can be found it is a tendency to near or above normal values. Indiana and Illinois show identical distributions in post El Niño harvests (2 below, 7 near, 8 above normal), with the Indiana results showing a significant tendency to near or above normal yields at a 91.34% confidence level and the Illinois results barely missing significance at a 90% confidence level. The slight differences in significance level can be traced to slight differences in the two state’s all-years yield distribution. Iowa and Nebraska show slight evidence of a tendency toward above normal yields, though not at a 90% confidence level. The distribution of Minnesota yields is close to the most probable values associ-

² Harvests of 1889, 1897, 1900, 1903, 1906, 1912, 1915, 1919, 1926, 1931, 1942, 1958, 1966, 1973, 1983, 1987, and 1992.

TABLE 2: Corn yields in years after El Niño winter periods

State	Harvests #	Below Normal	Near Normal	Above Normal	Significance %
Illinois					
After Warm Oct.-Feb.	17	2	<u>7</u>	<u>8</u>	89.96
All Years (1881-1994)	114	31	37	46	NA
Indiana					
After Warm Oct.-Feb.	17	2	<u>7</u>	<u>8</u>	91.34
All Years (1881-1994)	114	32	38	44	NA
Iowa					
After Warm Oct.-Feb.	17	5	4	<u>8</u>	77.81
All Years (1881-1994)	114	36	37	41	NA
Minnesota					
After Warm Oct.-Feb.	17	4	5	<u>8</u>	57.58
All Years (1881-1994)	114	30	36	48	NA
Nebraska					
After Warm Oct.-Feb.	17	4	4	<u>9</u>	83.23
All Years (1881-1994)	114	34	35	45	NA

Table 2. A test for a possible “post-El Niño phenomenon”. As in Table 1 for corn yields harvested in summers subsequent to 17 October-February periods marked by average S index conditions in the highest 17% ($S > +0.84$).

ated with chance sampling. As a result, there is no support here for the existence of such a post-El Niño phenomenon. If any relationship between El Niño events and corn yields is evident, it would be more properly termed a “pre-El Niño phenomenon”. That is, of the 12 warm SST JAS seasons selected in the skewness analyses leading to Table 1, all but two are consistent with pre-mature phase summer periods. Thus the majority of crops harvested after those summer seasons were harvested before mature El Niño conditions that occurred during the following winter months. Thus the results of Table 1 suggest a pre-El Niño boost in yields, particularly in Indiana, Illinois, and Minnesota.

c) Winter Wheat Yield Effects

In Appendix A the rainfall analysis for September-October-November (SON) indicates that wetter than normal conditions over Texas can occur as early as that season during El Niño periods, while Oklahoma, Kansas, and Nebraska may see abnormally wet conditions as early as December-January-February, assuming average S index conditions in the highest 17% during those three month periods. Conversely, the temperature and precipitation analyses of Appendix B imply shifts to warmer and drier winter conditions during La Niña periods. These La Niña climate responses are, again, conditional on anomalously cold SST conditions. Post-planting precipitation during the dormant period of winter wheat growth can have an important effect of soil moisture during the vegetative period and thus effect subsequent yield. In view of the evidence of above(below) normal winter-spring precipitation during the El Niño(La Niña) phase, the effects on winter wheat crops harvested subsequent to periods of mature ENSO conditions were analyzed. Whereas winter climate impacts over the major winter wheat producing regions of the central U.S. first appeared in the El Niño climate analyses during the DJF seasonal window, comparable effects in the La Niña analyses were first evident during November-December-January. As a result, the post-warm phase yield values sampled were those harvested after the 14 El Niño DJF periods of Fig. A7 that occurred during the period of available NASS winter wheat yield records (1909-1994), while the post-cold phase yields correspond to harvests after the 20 La Niña NDJ seasons of Fig. B6 that occurred over that same period.

Table 3 and Fig. 4 indicate a significant (95.4 %) tendency for above normal Kansas winter wheat yields after El Niño DJF periods. A significant (94.5%) incidence of below normal harvests after La Niña NDJ periods is also found in Kansas yields, indicating a positive correlation between winter SSTA and subsequent yields similar to that found for Illinois and Indiana corn. Similar linear yield effects are found over Texas, Oklahoma, and Colorado, with the Texas results showing the highest confidence levels. Of the 14 post-El Niño winter wheat harvests in Nebraska 7 were above normal, yet this sampling misses significance at a 90% confidence level. Sampling 20 post La Niña Nebraska yields and selecting 11 below normal is significant at a 94.5% confidence level. However, the incidence of above normal La Niña yields in Nebraska is close to the most probable value associated with random sampling, which suggests something other than a clear tendency for below normal values.

VI. DISCUSSION

a) Summer Climate and Yield Impacts

The effects of both ENSO phases on corn yield found here are in rough agreement with results reported by Handler (1984, 1990) and Carlson et al. (1996); i.e., that warm (cold) phase conditions tend to enhance (suppress) yields. However, while Handler's (1990) yield vs. SST correlations (his Fig. 3) suggest no significant relationship between SST during the growing season and yield, the results found here do show interpretable relationships linking SST and mid-western JAS climate to subsequent corn yield. In this regard, the relationships found here between SST during the growing season and yield are more in keeping with the results of Carlson et al. (1996), who conducted a yield analysis similar to that found here but based on the state of a Southern Oscillation surface pressure index (SOI) during June-July-August. Of the yield records from the five corn belt states considered here, three (Iowa, Illinois, and Indiana) were common to the analysis of Carlson et al. (1996). Although the relationships between yield and summer ENSO conditions found here

and in Carlson et al. (1996) are qualitatively similar, there are notable differences. Where they suggested an association between summers consistent with El Niño conditions and improved Iowa corn yield, no similar significant tendency was found here. Also, a tendency for near or below normal Indiana yields after cold SST summers was evident here (Table 1), but Carlson et al.'s (1996) distribution of below, near, and above trend Indiana yields during positive (> 0.8) SOI summers was consistent with chance sampling. The difference in the two corn yield analyses most likely stems from the fact that the SOI thresholds used by Carlson et al. (1996) and the SSTA thresholds used here do not define exactly equivalent ENSO states. As a result, the two analyses specified two sets of El Niño and La Niña summer periods that, although similar, are not exactly the same. However, it is emphasized that the yield analyses presented here are intended to be comparative in nature. The fact that both corn and winter wheat yield analyses have been derived using the same SST thresholds, the same statistical yardstick (i.e., hypergeometric statistics), and one criteria for statistical significance (i.e., a strict 90% significance threshold) makes these relative comparisons of yield effects valid.

The coincidence of the 1988/89 La Niña event and the summer drought of 1988 over the north central United States fueled speculation regarding a La Niña-drought connection. Some investigators (Trenberth et al. 1988; Palmer and Brancovic 1989) made the case for a cause and effect link between shifts in Pacific SST and northern hemisphere atmospheric circulation, and a resulting drought. On the other hand, Namias (1991) emphasized the local influence of dry soil moisture conditions during the spring of 1988. The most signifi-

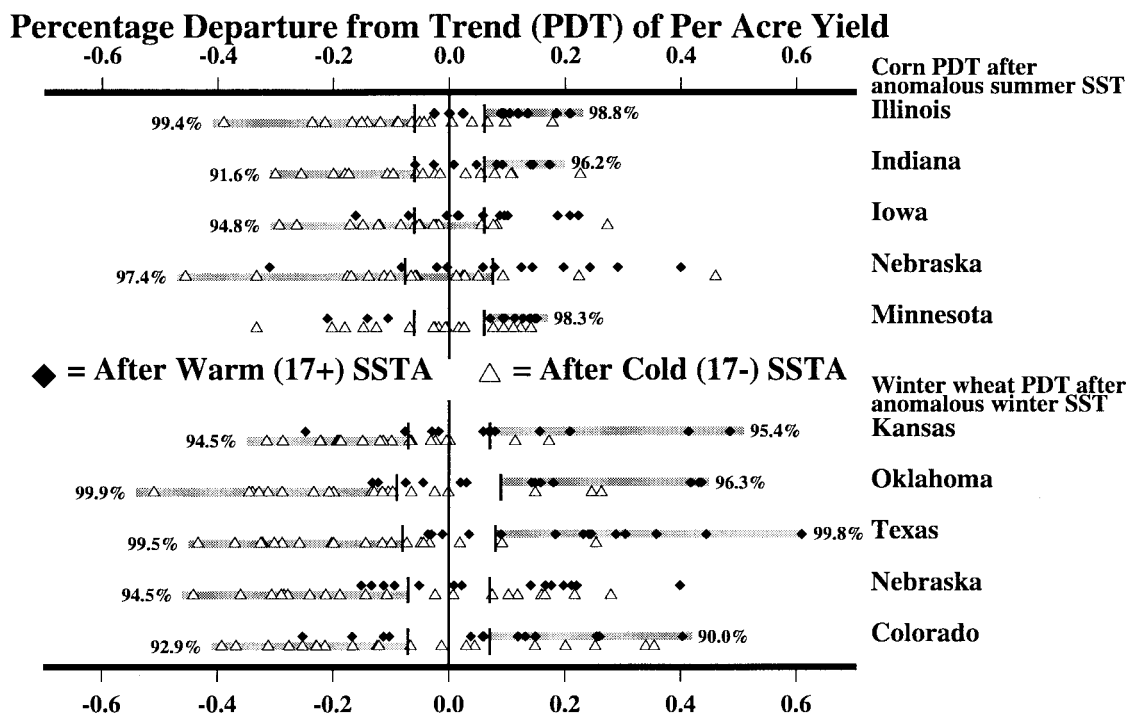


Fig. 4. Percentage Departure from Trend values (Eq. 2) for post ENSO per-acre corn and winter wheat yields in the states indicated. Diamond (Triangle) corn PDT values correspond to harvests immediately after JAS periods marked by mean S index values in the highest (lowest) 17% of the historical (1895-1997) distribution. Those values reproduce the distribution of below, near, and above normal 17+ and 17- entries in Table 1. Winter wheat PDT values marked by diamonds correspond to harvests after DJF seasons showing mean S index values in the highest 17%, and reproduce the distribution of below, near, and above normal 17+ entries in Table 3. Winter wheat PDT values marked by triangles correspond to harvests after NDJ periods marked by S index values in the lowest 17%, and reproduce the distribution of 17- entries in Table 3. Vertical lines mark near normal yield values for each state. Grey bars indicate skewness significant at 90% confidence level or better, and bar annotation shows associated significance level.

TABLE 3: Winter wheat yields after ENSO winter seasons

State	Harvests #	Below Normal	Near Normal	Above Normal	Significance %
Colorado					
After Warm DJF (17+)	14	4	3	<u>7</u>	90.5
After Cold NDJ (17-)	20	<u>11</u>	4	5	92.9
All Years (1909-1994)	86	33	26	27	NA
Kansas					
After Warm DJF (17+)	14	2	4	<u>8</u>	95.4
After Cold NDJ (17-)	20	<u>11</u>	7	2	94.5
All Years (1909-1994)	86	32	25	29	NA
Nebraska					
After Warm DJF (17+)	14	4	3	<u>7</u>	88.5
After Cold NDJ (17-)	20	<u>11</u>	2	7	94.5
All Years (1909-1994)	86	32	26	28	NA
Oklahoma					
After Warm DJF (17+)	14	2	4	<u>8</u>	96.3
After Cold NDJ (17-)	20	<u>14</u>	3	3	99.9
All Years (1909-1994)	86	31	27	28	NA
Texas					
After Warm DJF (17+)	14	0	4	<u>10</u>	99.8
After Cold NDJ (17-)	20	<u>13</u>	5	2	99.5
All Years (1909-1994)	86	32	26	28	NA

Table 3. As in Table 1 for post-ENSO winter wheat yields. “17+” entries show the number of total and below, near, and above normal per-acre yields of winter wheat after 14 December-January-February (DJF) periods marked by S index conditions in the highest 17%. “17-“ entries show the distribution of winter wheat yields after 20 November-December-January (NDJ) periods marked by S index conditions in the lowest 17%. “All years” entries indicate the distribution of yields for the (1909-1994) population of harvests for each state. Significance levels apply to the bold and underlined entries in each row.

cant summer cold phase climate effect found here is on temperature over the Midwest, but no significant accompanying effects on seasonal rainfall are apparent. Relaxing the local significance requirements for the rainfall analysis of cold phase JAS periods does show a more widespread tendency to dryness than is found in Fig. C2, but at a considerably lower confidence level (77.4%). However, climate divisions over Illinois and Indiana that show a coherent tendency to JAS temperatures in the highest 25% in Fig. C2 show no significant incidence of below median rainfall even at a more liberal confidence level. Thus a tendency to corn belt drought during strong La Niña conditions is not found here in the analysis of climate data. The unfavorable impacts on corn yield in Table 1 during periods of strong La Niña conditions might be due to the observed signal in JAS temperature, given the negative effects of heat stress alone on corn growth (Carlson, 1990).

However, Table 1 also shows significant tendencies to near or below normal corn yields in harvests after moderate and strong La Niña JAS periods, even though analyses of both JAS rainfall and temperature during “17-“ S index conditions (Fig. B2) show no significant skewness in climate. Thus adverse climate conditions are suggested – particularly in Illinois yields - even though no such evidence was found in the form of below median JAS rainfall or above median JAS temperature. A number of possible explanations might be offered for this. First, there is the possibility that the significantly reduced incidence of above normal “17-“ yields is due to stresses unrelated to weather, and that the coincidence with La Niña SST conditions is due to chance. In some cases the probability of this is fairly slim, though, as the Type I error of the “17-“ Illinois yield sampling in Table 1 is ~.5%. Assuming that climate-related stresses are to blame, the cause might be traced to the seasonal time resolution used here, or to conditioning the corn yield analyses on the state of July-August-September SST conditions. Regarding the first possibility, Carlson (1990) has shown that Iowa corn yields are sensitive to sub-seasonal (i.e., < 3 month) climate variability. For example, July temperature and heat stress were found to be significantly correlated with subsequent yield. Thus a hot July followed by normal or cool conditions in August and September could lead to reduced yields, but only marginally warm or even below median JAS seasonal temperature. Carlson’s (1990) results also show a significant dependence on July 1 soil moisture, thus only mildly adverse conditions during JAS may lead to decreased yields if rainfall prior to July is highly deficient. Yet given the highly significant connection between cold S index conditions during July-August-September and reduced Illinois yields, this implies a connection between JAS SST and Illinois rainfall prior to July 1. Such a connection may exist, but would not be apparent given the emphasis here on seasonally concurrent SST-climate conditions. Finally, there is the possibility that a significant incidence of hot or dry conditions over the Midwest were in fact present during the “17-“ JAS periods, but were poorly detected in station data. That is, it is possible that adverse weather effects were more accurately detected in the yields of a weather-sensitive crop harvested over an extensive and continuously planted region, than by relatively sparsely collected instrumental data. This suggests the interesting possibility that crop yield data might in some cases serve as a more sensitive proxy of climate than meteorological station data, particularly in the early portions of historical records in which data was collected from a widely scattered network of weather stations.

b) Winter Climate and Yield Impacts

When compared with the effects of both ENSO phases on summer climate over the central U.S., winter effects appear stronger and more coherent. Winter and spring fluctuations in precipitation and temperature appear more pronounced, as evident in the higher and more uniform incidence of extreme seasonal climate

conditions in the winter analyses of Appendices A and B when compared with the summer analyses. In addition, yield effects on winter wheat appear more consistent than the effects on corn yield. In Table 3 and Fig. 4 significant tendencies to below and above normal wheat yield effects are found in every state with the exception of post-warm phase Nebraska yields, which just miss significance at a 90% confidence level. In the corn yield analysis of Table 1, comparable results are found only in Indiana and Illinois. Results in other states either fail to meet the criteria of 90% significance or display a significant incidence of near or below normal trend values. As a result, the tendency to other than normal yield values after extreme ENSO periods appears stronger in the wheat yield results. With the exception of the post-warm phase Nebraska corn yields, the PDT values of the winter wheat yields in Fig. 4 are also more dispersed than that of corn. This is particularly clear in comparing the effects on post-warm phase yields. Table 1 shows a significant incidence to above normal corn yields in Illinois, Indiana, and Minnesota, but the associated PDT values in Fig. 4 are relatively modest (<0.2) when compared to the magnitude of post-warm phase wheat yield values in Kansas, Oklahoma, and Texas.

c) ENSO and the Potential for Seasonal Forecasts of Opportunity

Given the significant climate effects found here, the first condition for seasonal climate forecasting outlined in the Introduction appears to be satisfied over some portions of the Great Plains and Midwest during active ENSO periods. There is also evidence that the second condition is met; i.e., that the ENSO mechanism develops predictably over season-to-season time scales. Forecasting the state of equatorial Pacific SST has been a widely pursued research topic in both statistical and numerical forecasting (Zebiak and Cane 1987; Barnston and Ropelewski 1992; Barnett et al. 1993; Ji et al. 1994; Kirtman et al. 1997). The ability to forecast ENSO-related SST anomalies over 6 month lead times is described by Barnston et al. (1994) as moderate, with skill levels comparable to that of operational forecasts of midlatitude 500 mb height at 5-6 days lead time. Insofar as the ability to predict how ENSO-related sea-surface temperature will evolve over season-to-season time scales provides a measure of inherent predictability, the ENSO mechanism does show evidence of behaving predictably over those time scales. Although Barnston et al. (1994) also suggest that numerical models may not be meeting their full potential, the relative success of such models in forecasting the 1997-98 El Niño event (Kerr 1998) provides an encouraging hint that that potential may someday be realized. Future numerical forecasts of seasonal climate will most likely be attempted using a two stage approach (Bengtsson et al. 1993). The first stage involves predicting SST over inter-seasonal time scales, the second stage then uses the evolved SST state as a boundary condition on an Atmospheric General Circulation Model (AGCM) to determine climate effects over a subsequent seasonal time window. As discussed above, forecasts of ENSO-related sea-surface temperature anomalies exhibit moderate skill in forecasting inter-seasonal variability. Moreover, the numerical simulation experiments of Livezey et al. (1996) show that the ability of AGCMs to reproduce observed seasonal circulation over the Pacific-North American region is greatest during winter-spring periods consistent with mature ENSO conditions. Together, these developments suggest the future potential for numerically derived forecasts of opportunity during mature ENSO periods over the Pacific.

d) ENSO Forecasts of Opportunity and Agricultural Management

Assuming the potential for seasonal forecasts of opportunity, how valuable would they be to agricultural producers? One measure of usefulness is the degree to which such forecasts might influence planting decisions. An ideal situation might be one in which seasonal growing conditions were forecast prior to

planting. Sonka et al. (1982) suggest that higher application densities of seed and nitrogen may have increased 1979 Illinois corn yields by 21 bushels per acre, had the wet and relatively cool growing conditions of the summer of 1979 been known in advance. The tendency to wet and cool JAS periods found here during El Niño conditions suggests the possibility of forecasting favorable growth conditions over the corn belt. The ENSO-associated signal in winter-spring precipitation found here over Texas, Oklahoma, and Kansas also indicate climate effects that could potentially influence winter wheat planting decisions, as those effects occur after the September-October planting period. Thus a forecast of impending El Niño or La Niña conditions during the November-April period after planting might influence a cost-benefit analysis of planting winter wheat in these areas. In semi-arid portions of the Northern Plains where dryland farming is pursued, ENSO precipitation effects also have the potential of affecting spring wheat yields. Soil moisture conditions over eastern Montana and the western portion of the Dakotas are a determining factor in deciding whether to plant spring wheat or to withhold land from production to conserve soil moisture for a subsequent year's crop (Brown et al. 1986). The precipitation analyses presented here show a higher incidence of drier winter periods during mature El Niño conditions (Fig. A6-9), and La Niña winter periods show a significant tendency to wetter conditions over these regions (Fig. B6-7). However, these effects occur before the April-May planting period, thus the potentially predictable ENSO-related variation in soil moisture would be known before planting.

Another measure of value is the effect on net economic gain. This might be roughly measured by considering the cost-loss ratio analysis of Murphy (1985) in the context of ENSO forecasts of opportunity. Murphy (1985) assumes that the agricultural decision-maker chooses courses of action on a year-by-year basis that minimize expense. The expense associated with a particular course of action is the cost of protection against a climate threat, bounded by a maximum cost (C) providing full protection, plus the cost of climate-induced loss, bounded by a maximum possible degree of loss (L). Assuming a given C/L ratio, then the variables determining an optimal course of action are the probabilities associated with the upcoming growing season's climate conditions. Thus a low maximum protection cost and/or a potentially high cost of climate-induced loss, combined with a high probability of adverse growing conditions might lead a producer to invest in full protection. Conversely, a high protection cost and/or a low cost of loss, combined with a high probability of favorable growing conditions might lead a producer to forego protection altogether. Under conditions in which no known predictable climate mechanism is at work, seasonal forecasts are determined by climatological probability. Periodically, as during active ENSO periods, seasonal climate probabilities may shift significantly from those associated with climatology. As a consequence, optimal management strategies may change, with a potential for mitigating losses and increasing profitability during those periods.

VII. CONCLUSION

We propose that the potential for long-term economic gain derived from ENSO forecasts of opportunity may be greater for winter wheat producers than for corn producers for the following reasons. In the Introduction it was suggested that climate uncertainties make the pursuit of agriculture comparable to an ongoing game of chance. In addition it was proposed that predictable climate mechanisms such as ENSO may allow producers to anticipate a shift in the odds, the notion of which finds support in the results presented here. Although some conditional probabilities found here linking equatorial Pacific SST anomalies to concurrent seasonal climate are strong, they are not absolute. In addition, the two tiered forecasting schemes out-

lined above will introduce additional uncertainty through the SST forecast. Given that ENSO forecasts may reduce but not eliminate climate uncertainty, ENSO forecasts predicting seasonal growing conditions before planting might be compared to “loading the dice” in the farmer’s favor. But as even loaded dice behave with some degree of randomness, the potential for gain from ENSO forecasts of opportunity should not be measured based on the outcome a single cycle of forecast followed by an adjusted management strategy; i.e., a single “throw of the dice”. Instead, it should be based on the net outcome of a series of such cycles associated with ENSO events occurring periodically over an agricultural producer’s career. Considering the relatively sporadic occurrence of ENSO events, the use of ENSO forecasts in long-term management might be compared to being given occasional access to loaded dice in agriculture’s ongoing gambling situation. The suggestion made here is that producers of winter wheat may be offered such dice more frequently, and that they may be more heavily weighted towards certain climate and yield outcomes. This is based on the following observations:

- ◆ Higher frequency of winter ENSO activity is evident in Figs. 1a and b, and in the greater number of winter seasons meeting extreme S index conditions in Figs. A6 (25) and B6 (22) when compared with the summer analyses of Fig. A2 (13) and Fig. B2 (14). Fully developed ENSO conditions are primarily a feature of northern winter, with northern summer periods typically associated with initial or final stages of event development. Thus while anomalous northern winter conditions are characteristic of most ENSO events, only certain events develop quickly enough, or persist long enough, to produce anomalous northern summer conditions.
- ◆ More reliable winter ENSO forecasts might be implied in the higher levels of significance in skewness about the median, and the incidence of extreme seasonal climate conditions in the winter analyses in Appendices A and B when compared with the analyses of Figs. A2 and C2. This is most likely due to the increased incidence of extreme warm and cold SSTA conditions during October-February, a period of peak ENSO strength. Sea-surface temperature anomalies in the highest and lowest 10% of the historical distribution are consistent with stronger coupling between the oceanic and atmospheric components of ENSO, and more robust effects on midlatitude atmospheric circulation.
- ◆ Regarding yield outcomes, the tendency to other than normal yields in Tables 1 and 3 is generally more significant in the winter wheat results, and the patterns of significance highlighted in Fig. 4 show a more uniform and greater magnitude of effect on wheat yield. It is worth noting that the strongest effects evident in Tables 1 and 3 and Fig. 4 is on a crop dependent on winter precipitation and grown in the southernmost part of the study region; i.e., the impacts on winter wheat yields in Texas.

The intent, though, is not to suggest that ENSO forecasts of opportunity will not be useful in corn production in the long term. One factor not accounted for here, the relative worth of the U.S. corn crop compared to the winter wheat crop, may favor corn producers. That is, while it is possible that the ENSO mechanism may affect summer growing conditions on a less frequent basis in the long term, the economic returns involved – the “stakes” in the gambling analogy – may be much greater.

As the winter climate effects found here extend across lower latitude areas of the continental United States, strong yield impacts might also occur in crops not considered here. Schonher and Nicholson's (1989) study of the effects of the El Niño phase on California rainfall shows a significant tendency to above average annual rainfall in the southern portion of that state, which is also indicated here in the precipitation analyses of Figs. A7-9. Anecdotal evidence of warm phase effects on agriculture in this region might be found in the impact of the 1997/98 El Niño event on the winter romaine lettuce crop (Associated Press 1998). Heavy rains associated with that event led to delays in planting, seedling mortality, and fungus infestation due to standing water in the fields. The negative effects on yield might be inferred from the resulting increase in wholesale prices from \$10 to \$50 per case. The use of ENSO forecasts to anticipate effects on agricultural production may be also be possible in regions such as the Rio Grande River Valley and Florida, where ENSO-related rainfall effects are apparent and winter produce crops are cultivated and harvested during seasons of peak ENSO activity. Abnormally wet conditions over Florida during the spring of 1998 led to delays in harvesting, planting and fieldwork (Weekly Weather and Crop Bulletin 1998). These examples suggest the possibility that the previous discussion regarding the value of ENSO forecasts may be more broadly applied; i.e., that the potential for long-term economic gain over the continental U.S. may be greater for winter crops than for summer crops in general.

Acknowledgements: Thanks to Cathy Lester and Adela Ramirez of the USDA/ARS Cropping Systems Research Lab at Big Spring TX for editorial suggestions and for converting this report to PDF. With the exception of Figure 1 and Figure 2a, all figures were produced with Generic Mapping Tools (Wessel and Smith, 1995).

WORLD WIDE WEB RESOURCES

A number of web sites (active as of February 1999) provide up to date information regarding the current state of the ENSO mechanism and experimental forecasts of ENSO-related sea-surface temperature conditions. The United States Government's primary site addressing these issues originates from Climate Prediction Center (CPC).

http://nic.fb4.noaa.gov:80/products/analysis_monitoring/ensostuff/index.html

The CPC reports information regarding monthly mean SST conditions averaged over four regions of the eastern and central equatorial Pacific. These are the Niño 1+2, 3, 3.4, and 4 regions. It was found here that Wright's (1989) S index was most highly correlated with Niño 3 ($r = .949$) and Niño 3.4 ($r = .952$) sea-surface temperature anomalies over the period 1950-1986.

<http://nic.fb4.noaa.gov:80/data/cddb/cddb/sstoi.indices>

The University of California's Scripps Institute of Oceanography also issues experimental forecasts of ENSO SST conditions.

<http://meteora.ucsd.edu/~pierce/elnino/elnino.html>

The National Oceanographic and Atmospheric Administration's Pacific Marine Environmental Lab (PMEL) maintains a web page with links to other sites:

<http://www.pmel.noaa.gov/toga-tao/el-nino/>

REFERENCES

- “Heads up, lettuce lovers – romaine crop takes a blow from El Niño”. Associated Press, May 6, 1998.
- Allan, R., J. Lindesay, and D. Parker, 1996: *El Niño Southern Oscillation and Climate Variability*. CSIRO, Australia.
- Barnett, T.P., and Coauthors, 1993: ENSO and ENSO-related predictability. Part I – Prediction of equatorial Pacific sea-surface temperatures with a hybrid coupled ocean-atmosphere model. *J. Climate*, **6**, 1545-1566.
- Barnston, A.G., R.E. Livezey, and M.S. Halpert, 1991: Modulation of Southern Oscillation-Northern Hemisphere mid-winter climate relationships by the QBO. *J. Climate*, **4**, 203-217.
- Barnston, A.G. and C.F. Ropelewski, 1992: Prediction of ENSO episodes using canonical correlation analysis. *J. Climate*, **5**, 1316-1345.
- Barnston, A.G., H.M. van den Dool, S.E. Zebiak, T.P. Barnett, M. Ji, D.R. Rodenhuis, M.A. Cane, A. Leetma, N.E. Graham, C.R. Ropelewski, V.E. Kousky, E. O’Lenic and R.E. Livezey, 1994: Long lead seasonal forecasts - where do we stand? *Bull. Amer. Meteor. Soc.*, **75**, 2097-2114.
- Bengtsson, L., U. Schlese, E. Roeckner, M. Latif, T.P. Barnett, and N. Graham, 1993: A two-tiered approach to long range climate forecasting. *Science*, **261**, 1026-1029.
- Brown, B.G., R.W. Katz, and A.H. Murphy, 1986: On the economic value of seasonal-precipitation forecasts: The following/planting problem. *Bull. Amer. Meteor. Soc.*, **67**, 833-841.
- Bunkers, M.J., J.R. Miller Jr., and A.T. DeGaetano, 1996: An examination of El Niño – La Niña related precipitation and temperature anomalies across the Northern Plains. *J. Climate*, **9**, 147-160.
- Carlson, R.E, 1990: Heat stress, plant-available soil moisture, and corn yields in Iowa: A short and long term view. *Journal of Production Agriculture*, **3**, 293-297.
- Carlson, R.E, D.P. Todey, and S.E. Taylor, 1996: Midwestern corn yield and weather in relation to extremes of the Southern Oscillation. *Journal of Production Agriculture*, **9**, 347-352.
- Duchon, C.E., 1977: Lanczos filtering in one and two dimensions. *J. Appl. Meteor.*, **18**, 1016-1022.
- Garnett, E.R., and M.D. Khandekar, 1992: The impact of large-scale atmospheric circulations and anomalies on Indian monsoon droughts and floods and on world grain yields - a statistical analysis. *Agricultural and Forest Meteorology*, **61**, 113-128.
- Guttman, N.B., and R.G. Quayle, 1996: A historical perspective of U.S. climate divisions. *Bull. Amer. Meteor. Soc.*, **77**, 293-303.
- Handler, P., 1984: Corn yields in the United States and sea-surface temperature anomalies in the equatorial Pacific Ocean during the period 1868-1982. *Agricultural and Forest Meteorology*, **31**, 25-32.
- Handler, P., 1990: USA corn yields, the El Niño and agricultural drought: 1867-1988. *International J. Climatol.*, **10**, 819-828.
- Hoerling, M.P., A. Kumar, and M. Zhong, 1997: El Niño, La Niña, and the nonlinearity of their teleconnections. *J. Climate*, **10**, 1769-1786.
- Ji, M., A. Kumar and A. Leetma, 1994: A multi-season climate forecast system at the National Meteorological Center. *Bull. Amer. Meteor. Soc.*, **75**, 569-577.

- Kerr, R.A., 1998: Models win big in forecasting El Niño. *Science*, **280**, 522-523.
- Kirtman B.P., P.J. Shukla, B. Huang, Z. Zhu, and E.K. Schneider, 1996: Multi-season predictions with a coupled tropical ocean global atmosphere system. *Mon. Wea. Rev.*, **125**, 789-808.
- Livezey, R.E., M. Masutani and Ming Ji, 1996: SST-forced seasonal simulation and prediction skill for versions of the NCEP/MRF model. *Bull. Amer. Met. Soc.*, **77**, 507-517.
- Livesey, R.E., M. Masutani, A. Leetma, H. Rui, Ming Ji, and A. Kumar, 1997: Teleconnective response of the Pacific-North American region atmosphere to large central equatorial Pacific SST anomalies. *J. Climate*, **10**, 1787-1820.
- Mauget, S.A. and D.R. Upchurch, 1999: El Niño and La Niña related climate and agricultural impacts over the continental United States. Accepted by the *Journal of Production Agriculture*.
- Mendenhall, W., D.D. Wackerly and R.L. Scheaffer, 1990: *Mathematical Statistics with Applications*. 4th ed. PWS-Kent, Boston, 818 pp.
- Mjelde, J.W., and K. Keplinger, 1998: Using the Southern Oscillation to forecast Texas winter wheat and sorghum crop yields. *J. Climate*, **11**, 54-60.
- Montroy, D.L., 1997: Linear relation of central and eastern North American precipitation to tropical Pacific sea surface temperature anomalies. *J. Climate*, **10**, 541-558.
- Murphy, A.H., 1985: Decision making and the value of forecasts in a generalized model of the cost-loss ratio situation. *Mon. Wea. Rev.*, **113**, 362-369.
- Namias, J., 1991: Spring and summer 1988 drought over the contiguous United States – causes and predictions. *J. Climate*, **4**, 54-65.
- Palmer, T.N. and C. Brancovic, 1989: The 1988 U.S. drought linked to anomalous sea surface temperature. *Science*, **338**, 54-57.
- Philander, S.G., 1990: *El Niño, La Niña and the Southern Oscillation*. Academic Press, San Diego.
- Rasmusson, E.M. and T.H. Carpenter, 1982: Variations in tropical sea surface temperature and surface wind fields associated with the Southern Oscillation/El Niño. *Mon. Wea. Rev.*, **110**, 354-383.
- Ropelewski, C.F. and M.S. Halpert, 1986: North American precipitation and temperature patterns associated with the El-Niño/Southern Oscillation (ENSO). *Mon. Wea. Rev.*, **114**, 2352-2362.
- Ropelewski, C.F. and M.S. Halpert, 1989: Precipitation patterns associated with the high index phase of the Southern Oscillation. *J. Climate*, **2**, 268-283.
- Schonher, T. and S.E. Nicholson, 1989: The relationship between California rainfall and ENSO events. *J. Climate*, **2**, 1258-1269.
- Sonka, S.T., P.J. Lamb, S.A. Changnon Jr, and A. Wiboonpongse, 1982: Can climate forecasts for the growing season be valuable to crop producers: Some general considerations and an Illinois plot study. *J. Appl. Meteor.*, **21**, 471-476.
- Trenberth, K.E., 1991: General characteristics of the El Niño-Southern Oscillation. *Teleconnections Linking Worldwide Climate Anomalies*, M.H. Glantz, R.W. Katz, and N. Nicholls, Eds. Cambridge University Press, 13-42.

- Trenberth, K.E., G.W. Branstator and P.A. Arkin, 1988: Origins of the 1988 North American drought. *Science*, **242**, 1640-1645.
- Trenberth, K.E. and D.J. Shea, 1987: On the evolution of the Southern Oscillation. *Mon. Wea. Rev.*, **115**, 3078-3096.
- Weekly Weather and Crop Bulletin. March, 31, 1998. Joint Agricultural Weather Facility, USDA-WAOB, Wash. D.C.
- Wessel, P. and W.H.F. Smith, 1995: New version of the Generic Mapping Tools Released. *EOS Transactions American Geophysical Union*, **76**, 329.
- Wilks, D.S., 1995: *Statistical Methods in the Atmospheric Sciences*. Academic Press, San Diego, 464 pp.
- Wright, P.B., 1989: Homogenized long-period Southern Oscillation indices. *International J. Climatol.* **9**, 33-54.
- Zebiak, S.E., and M.A. Cane, 1987: A model El Niño-Southern Oscillation. *Mon. Wea. Rev.*, **115**, 2262-2278.

APPENDIX A

Figures A1-A10 show statistical analyses of cumulative rainfall (a) and mean temperature (b) for 3 month seasonal periods during which the average value of Wright's S index (Wright, 1989) was in the highest 17% ($> +0.84$ C) of 1895-1997 values. The listed years refer to the years in which the first month of the 3 month periods fell, thus NDJ 1896 refers to November-December-January of 1896/97. Shaded (hatched) climate divisions indicate areas that experienced a significant incidence of above (below) median seasonal climate. Confidence levels for skewness about the median can be found under the greyscale legend. Where climate divisions are annotated, a significant incidence of seasonal climate in the lowest or highest 25% of historical values was found, with (n/m) indicating n seasons in the lowest 25%, m seasons in the highest 25%.

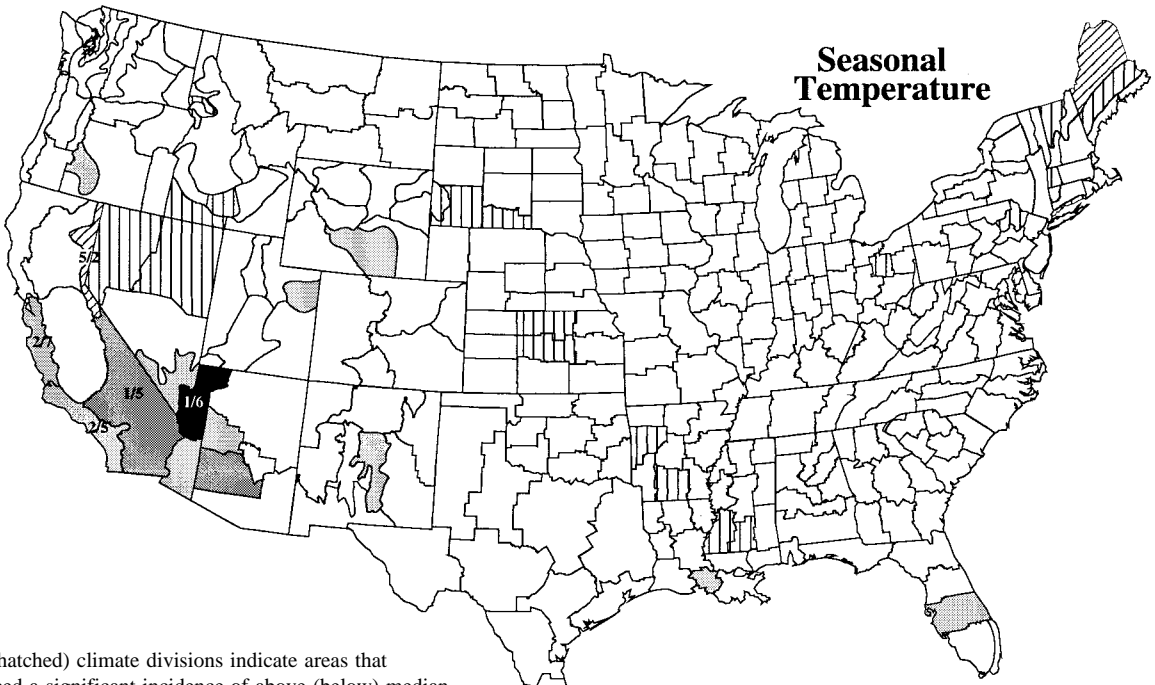
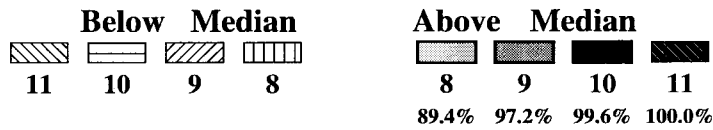
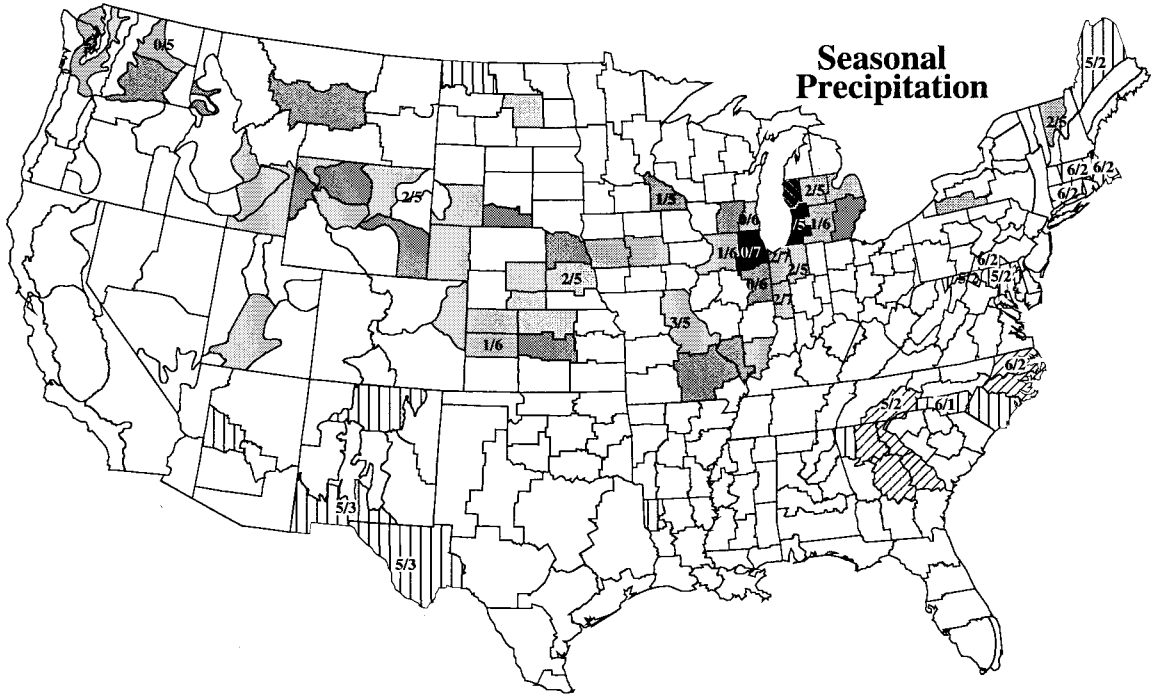
El Niño Precipitation and Temperature Analyses

Summer-Fall	June-July-August (JJA)	Figure A1
	July-August –September (JAS)	A2
	August –September-October (ASO)	A3
Fall-Winter	September-October-November (SON)	A4
	October-November-December (OND)	A5
	November-December-January (NDJ)	A6
	December-January –February (DJF)	A7
Winter-Spring	January –February –March (JFM)	A8
	February –March-April (FMA)	A9
	March-April-May (MAM)	A10
	April-May-June (AMJ)	A11

Figure A1: El Niño June-July-August

11 seasons

- 1896
- 1900
- 1902
- 1905
- 1957
- 1965
- 1972
- 1982
- 1983
- 1987
- 1997

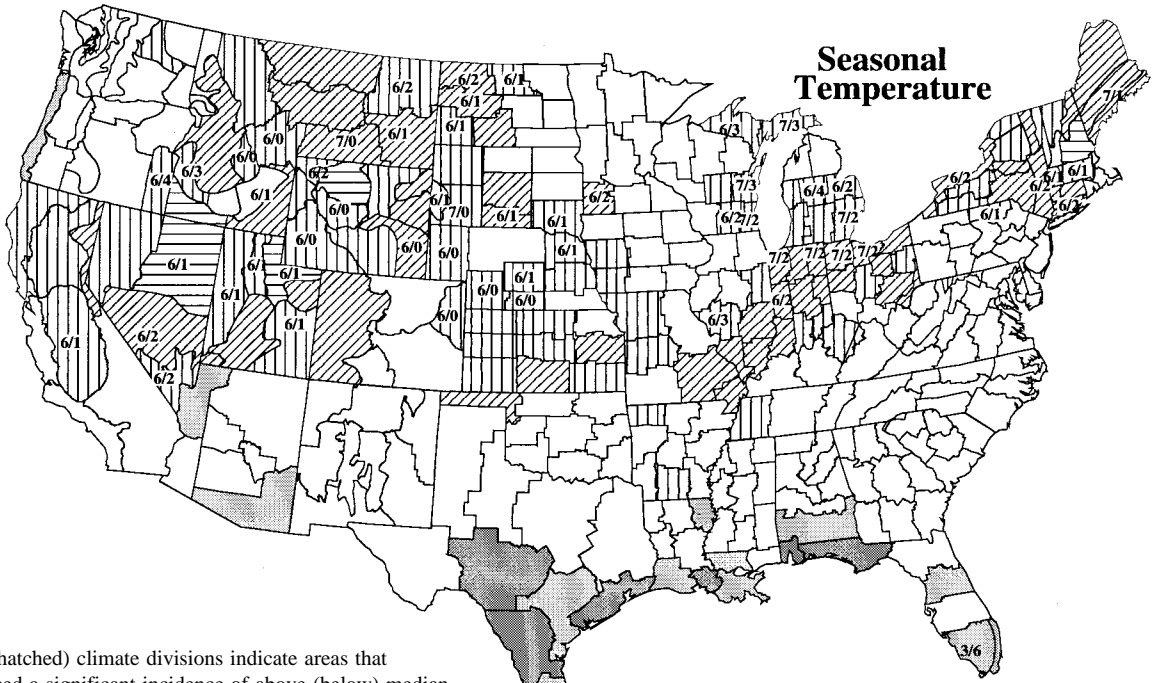
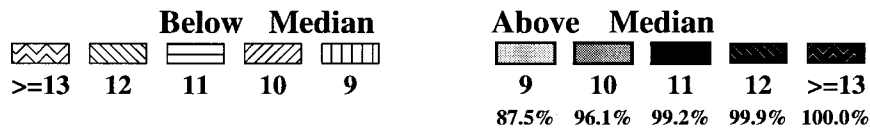
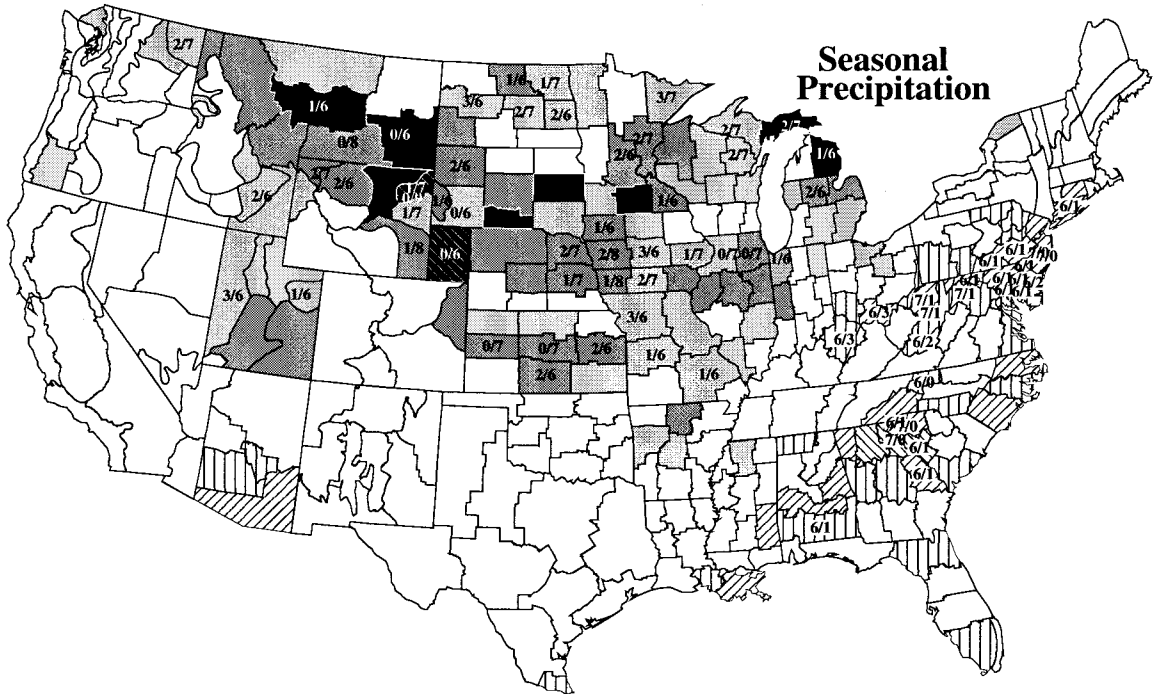


Shaded (hatched) climate divisions indicate areas that experienced a significant incidence of above (below) median seasonal climate. Confidence levels for skewness about the median can be found under the greyscale legend. Where climate divisions are annotated, a significant incidence of seasonal climate in the lowest or highest 25% of historical values was found, with (n/m) indicating n seasons in the lowest 25%, m seasons in the highest 25%.

Figure A2: El Niño July-August-September

13 seasons

- 1896
- 1900
- 1902
- 1905
- 1918
- 1941
- 1951
- 1957
- 1965
- 1972
- 1982
- 1987
- 1997

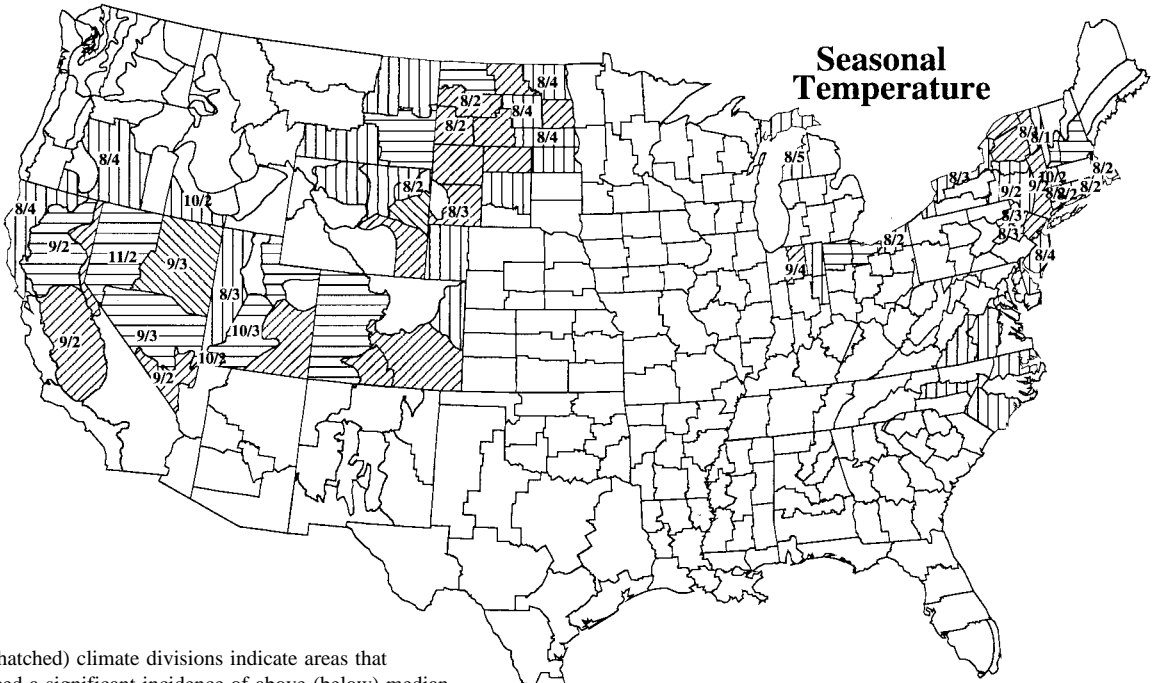
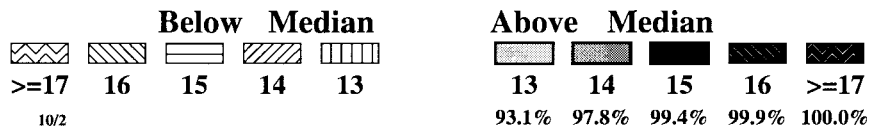
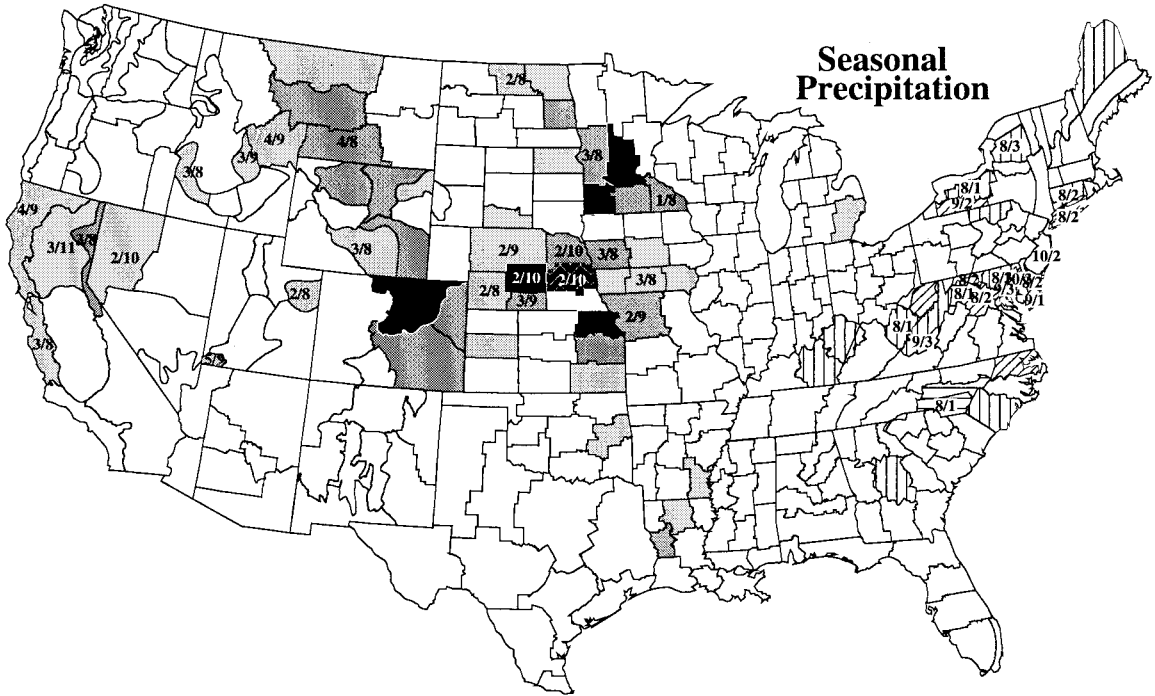


Shaded (hatched) climate divisions indicate areas that experienced a significant incidence of above (below) median seasonal climate. Confidence levels for skewness about the median can be found under the greyscale legend. Where climate divisions are annotated, a significant incidence of seasonal climate in the lowest or highest 25% of historical values was found, with (n/m) indicating n seasons in the lowest 25%, m seasons in the highest 25%.

Figure A3: El Niño August-September-October

19 seasons

- 1896
- 1899
- 1900
- 1902
- 1904
- 1905
- 1911
- 1914
- 1918
- 1930
- 1940
- 1941
- 1951
- 1957
- 1965
- 1972
- 1982
- 1987
- 1997

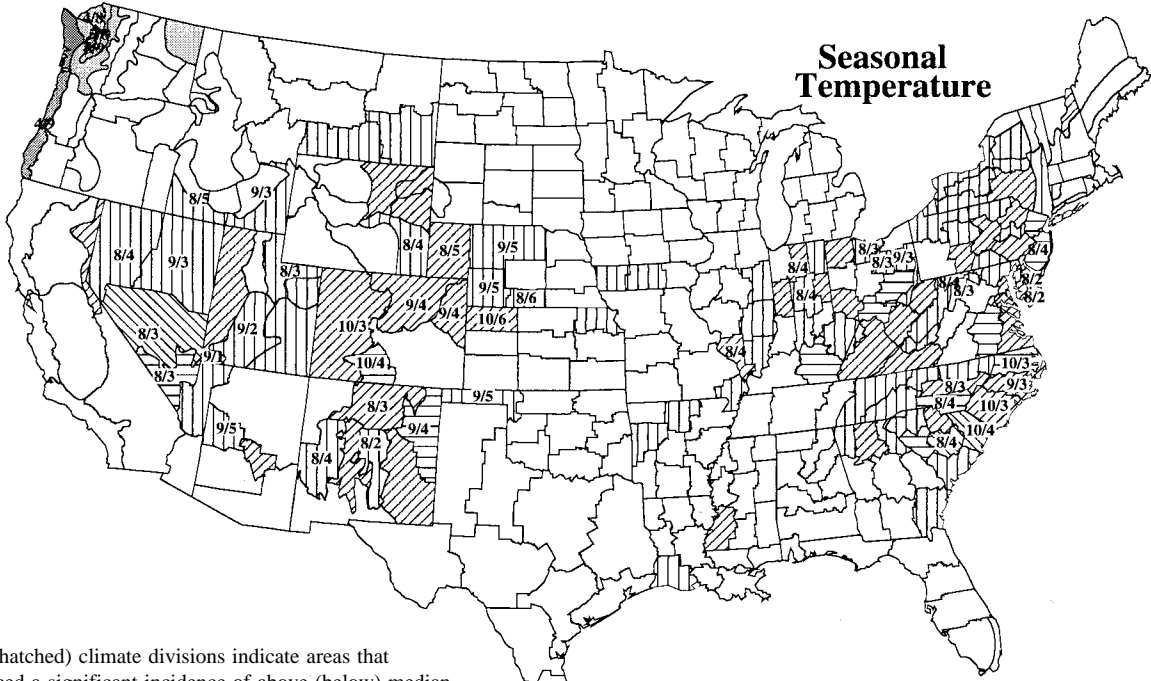
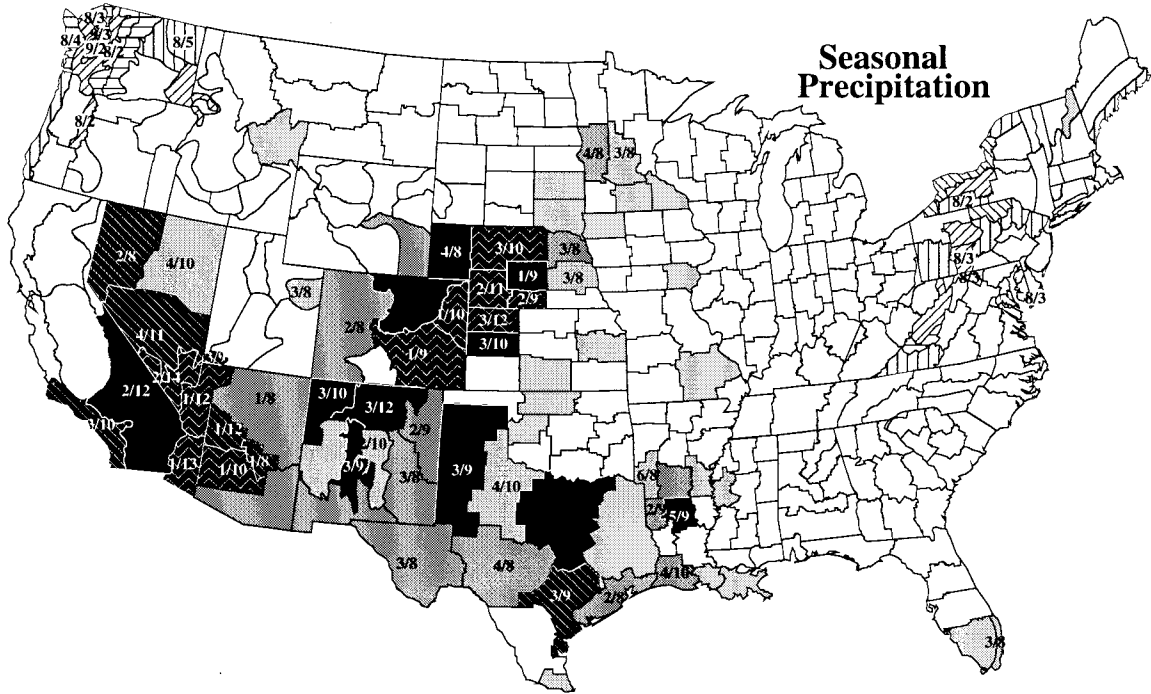


Shaded (hatched) climate divisions indicate areas that experienced a significant incidence of above (below) median seasonal climate. Confidence levels for skewness about the median can be found under the greyscale legend. Where climate divisions are annotated, a significant incidence of seasonal climate in the lowest or highest 25% of historical values was found, with (n/m) indicating n seasons in the lowest 25%, m seasons in the highest 25%.

Figure A4: El Niño September-October-November

22 seasons

- 1896
- 1899
- 1902
- 1904
- 1905
- 1911
- 1914
- 1918
- 1923
- 1930
- 1940
- 1941
- 1951
- 1957
- 1963
- 1965
- 1969
- 1972
- 1976
- 1982
- 1987
- 1991

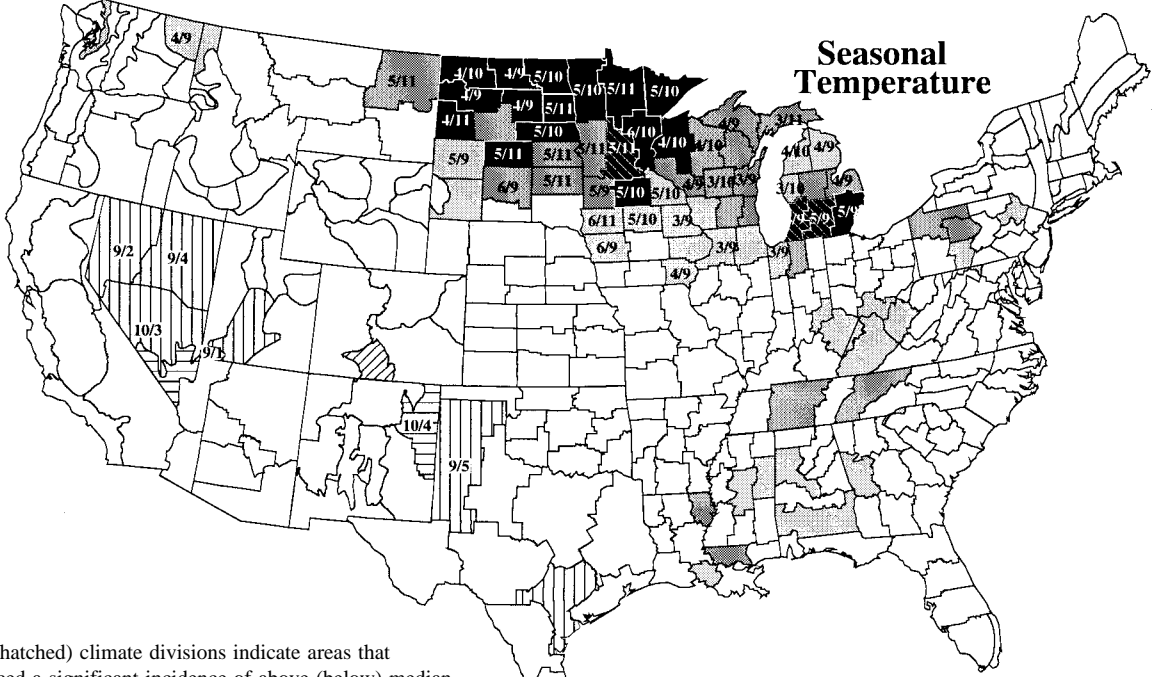
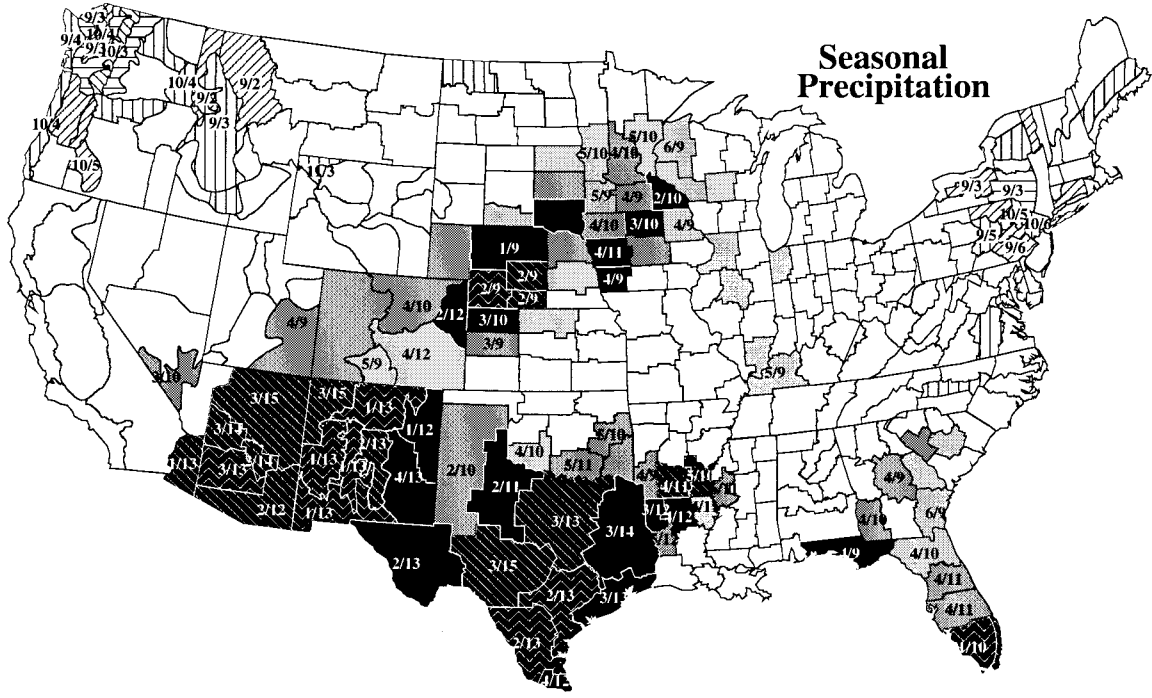


Shaded (hatched) climate divisions indicate areas that experienced a significant incidence of above (below) median seasonal climate. Confidence levels for skewness about the median can be found under the greyscale legend. Where climate divisions are annotated, a significant incidence of seasonal climate in the lowest or highest 25% of historical values was found, with (n/m) indicating n seasons in the lowest 25%, m seasons in the highest 25%.

Figure A5: El Niño October-November-December

25 seasons

- 1896
- 1899
- 1902
- 1904
- 1905
- 1911
- 1914
- 1918
- 1923
- 1925
- 1930
- 1939
- 1940
- 1941
- 1951
- 1957
- 1963
- 1965
- 1969
- 1972
- 1982
- 1986
- 1987
- 1991
- 1994

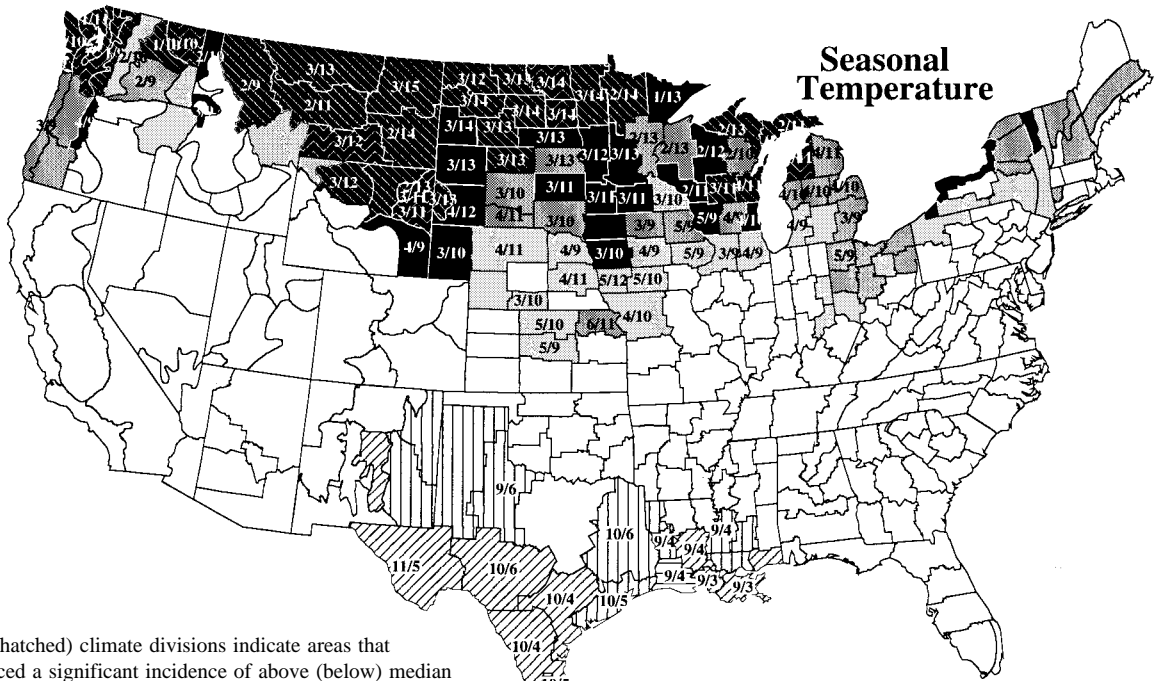
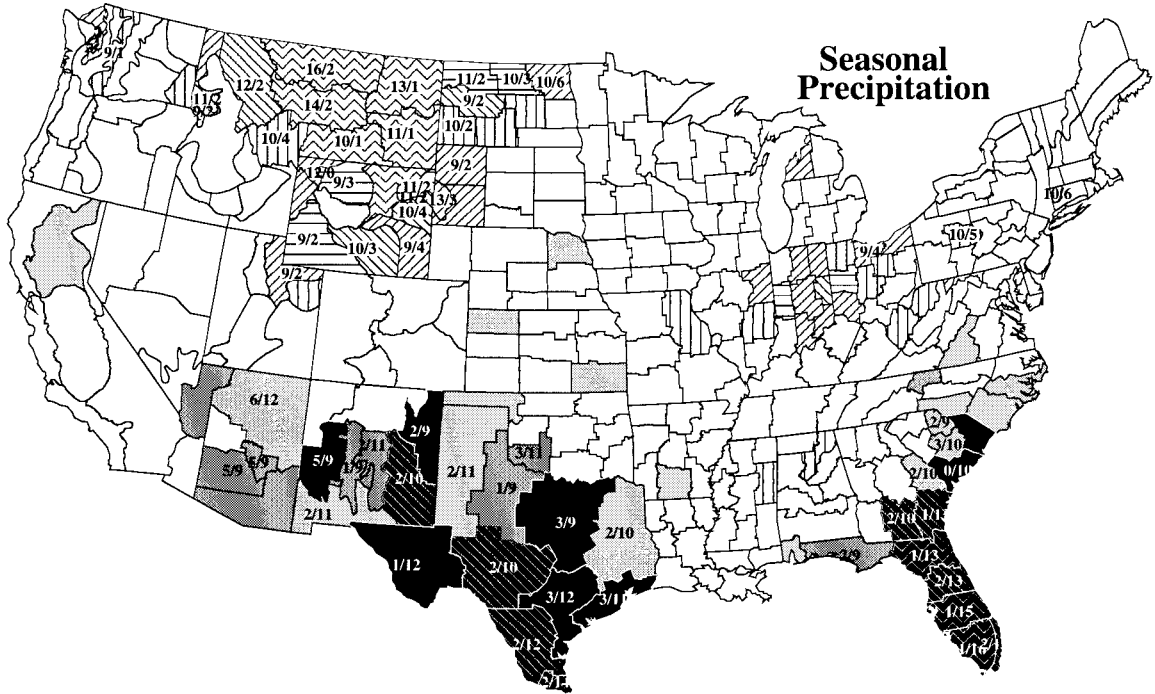


Shaded (hatched) climate divisions indicate areas that experienced a significant incidence of above (below) median seasonal climate. Confidence levels for skewness about the median can be found under the greyscale legend. Where climate divisions are annotated, a significant incidence of seasonal climate in the lowest or highest 25% of historical values was found, with (n/m) indicating n seasons in the lowest 25%, m seasons in the highest 25%.

Figure A6: El Niño November-December-January

25 seasons

- 1896
- 1899
- 1902
- 1904
- 1905
- 1911
- 1913
- 1914
- 1918
- 1925
- 1930
- 1939
- 1940
- 1941
- 1951
- 1957
- 1963
- 1965
- 1969
- 1972
- 1982
- 1986
- 1987
- 1991
- 1994

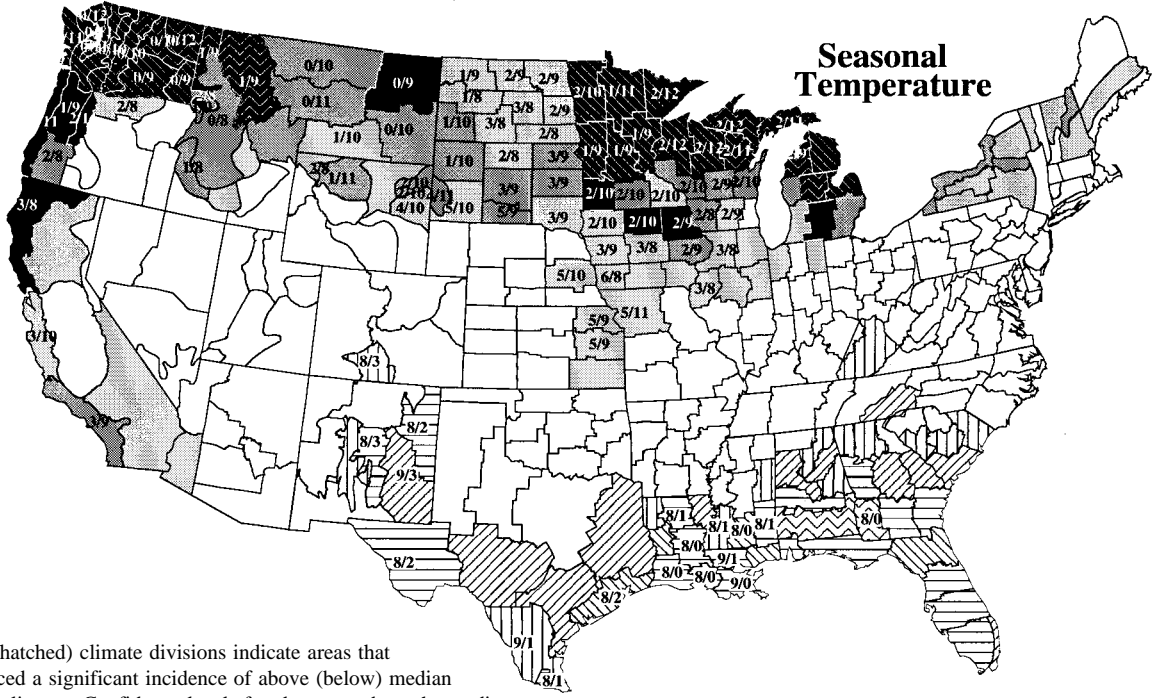
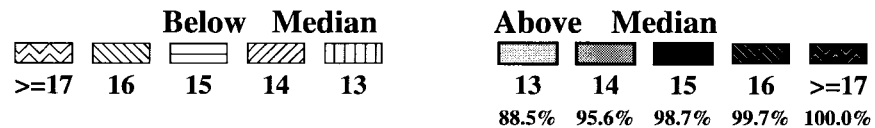
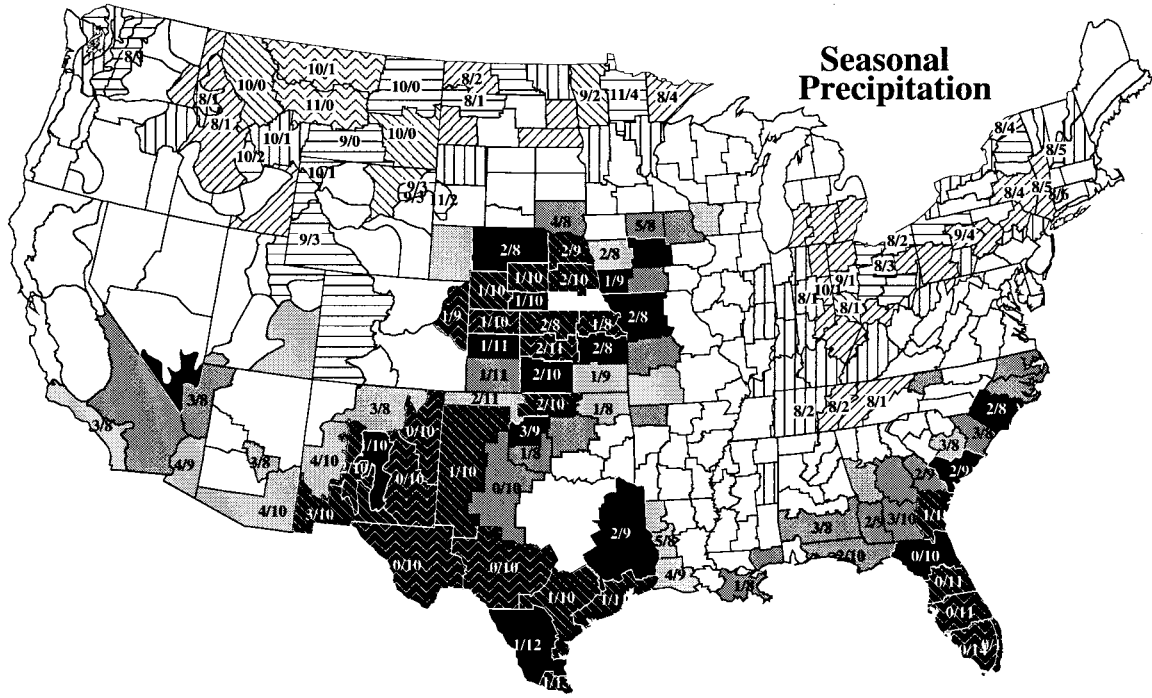


Shaded (hatched) climate divisions indicate areas that experienced a significant incidence of above (below) median seasonal climate. Confidence levels for skewness about the median can be found under the greyscale legend. Where climate divisions are annotated, a significant incidence of seasonal climate in the lowest or highest 25% of historical values was found, with (n/m) indicating n seasons in the lowest 25%, m seasons in the highest 25%.

Figure A7: El Niño December-January-February

20 seasons

- 1896
- 1899
- 1902
- 1904
- 1905
- 1911
- 1913
- 1914
- 1918
- 1925
- 1930
- 1939
- 1940
- 1957
- 1965
- 1972
- 1982
- 1986
- 1991
- 1994

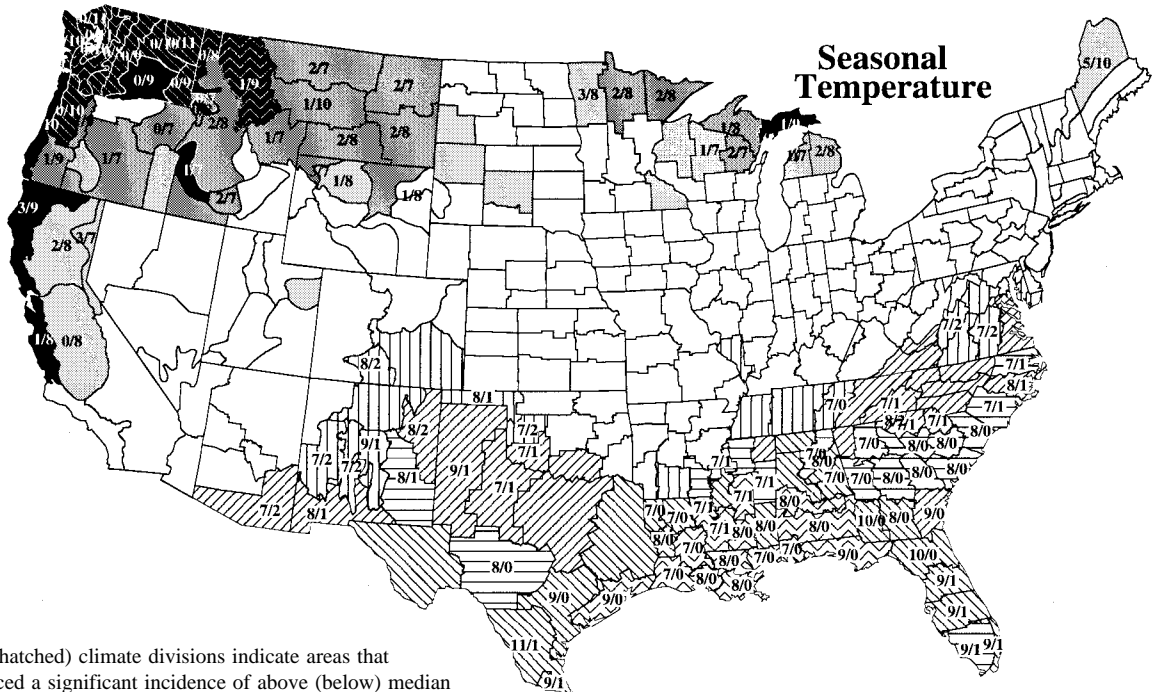
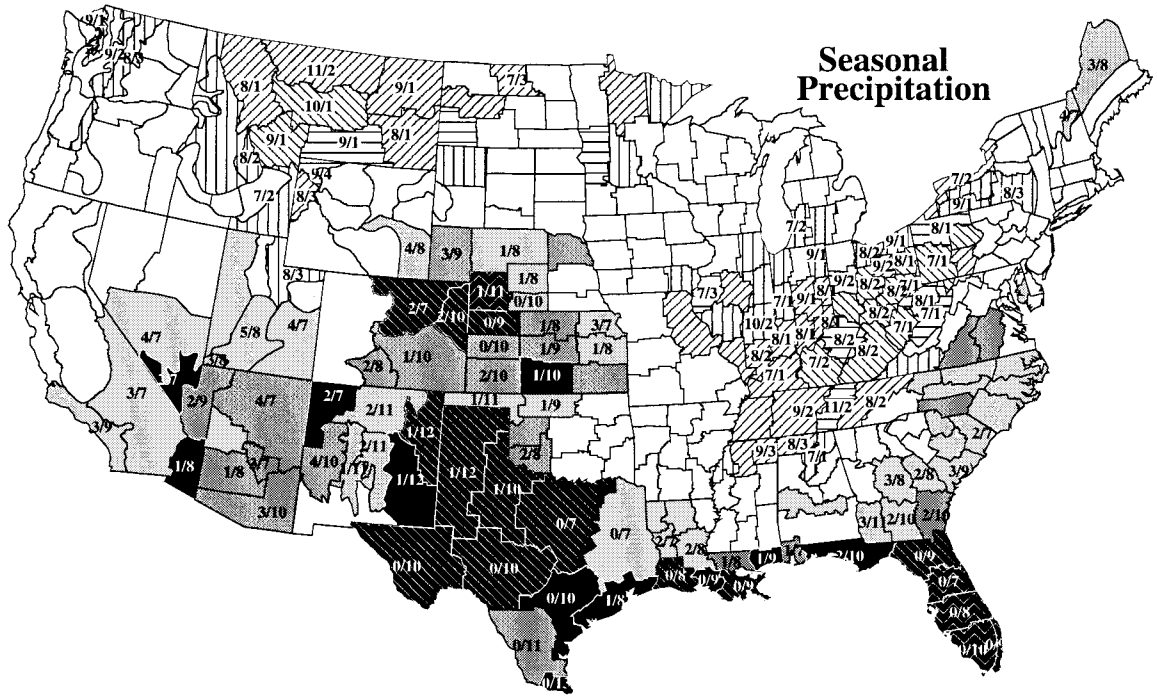


Shaded (hatched) climate divisions indicate areas that experienced a significant incidence of above (below) median seasonal climate. Confidence levels for skewness about the median can be found under the greyscale legend. Where climate divisions are annotated, a significant incidence of seasonal climate in the lowest or highest 25% of historical values was found, with (n/m) indicating n seasons in the lowest 25%, m seasons in the highest 25%.

Figure A8: El Niño January-February-March

18 seasons

- 1897
- 1900
- 1903
- 1905
- 1906
- 1912
- 1914
- 1915
- 1919
- 1926
- 1931
- 1941
- 1958
- 1966
- 1973
- 1983
- 1987
- 1992

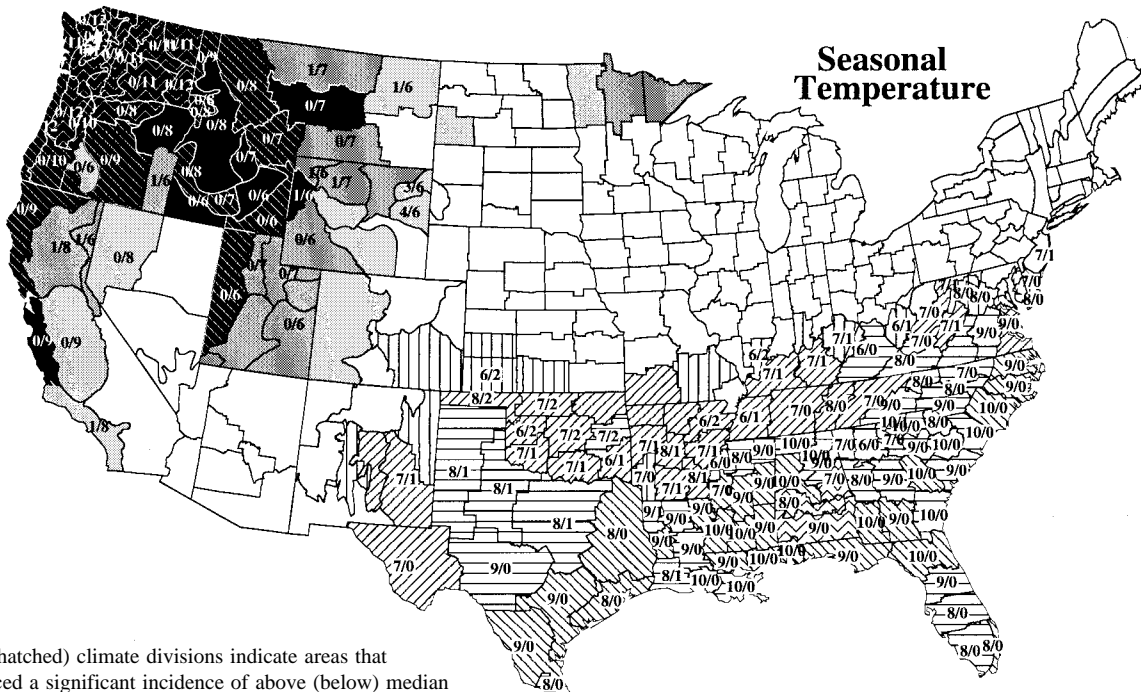
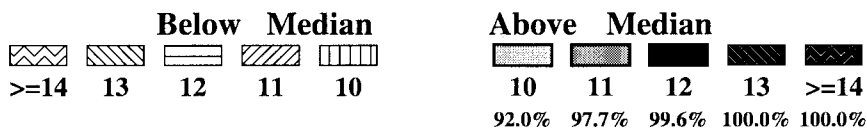
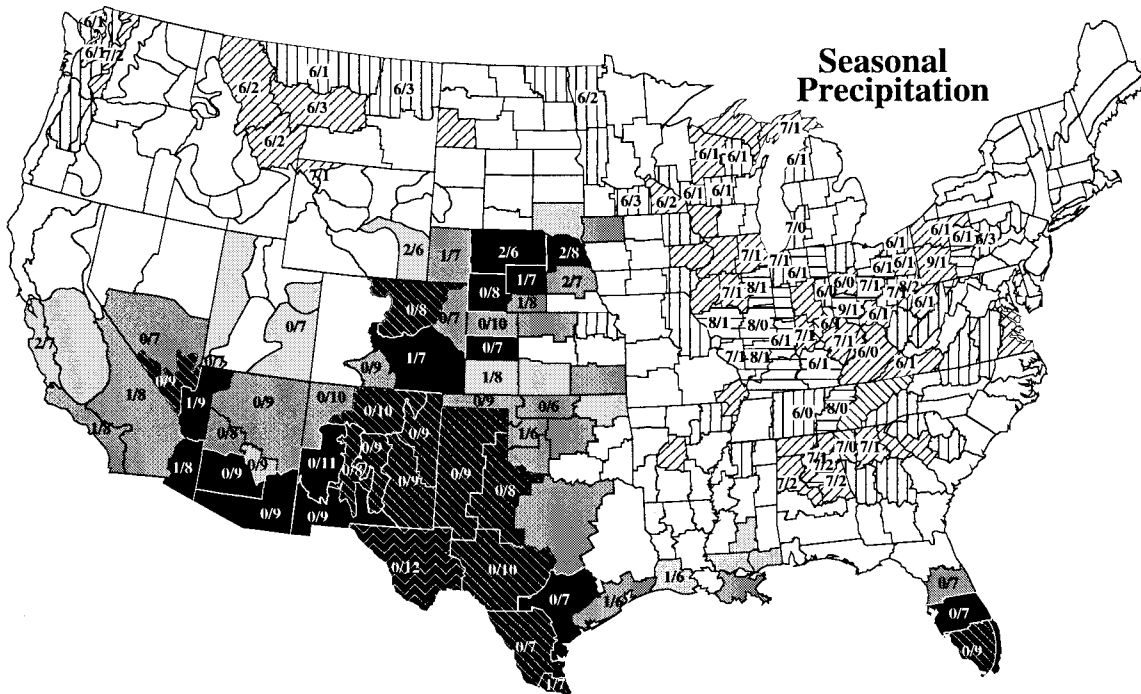


Shaded (hatched) climate divisions indicate areas that experienced a significant incidence of above (below) median seasonal climate. Confidence levels for skewness about the median can be found under the greyscale legend. Where climate divisions are annotated, a significant incidence of seasonal climate in the lowest or highest 25% of historical values was found, with (n/m) indicating n seasons in the lowest 25%, m seasons in the highest 25%.

Figure A9: El Niño February-March-April

14 seasons

- 1900
- 1905
- 1906
- 1914
- 1915
- 1919
- 1926
- 1931
- 1940
- 1941
- 1958
- 1983
- 1987
- 1992

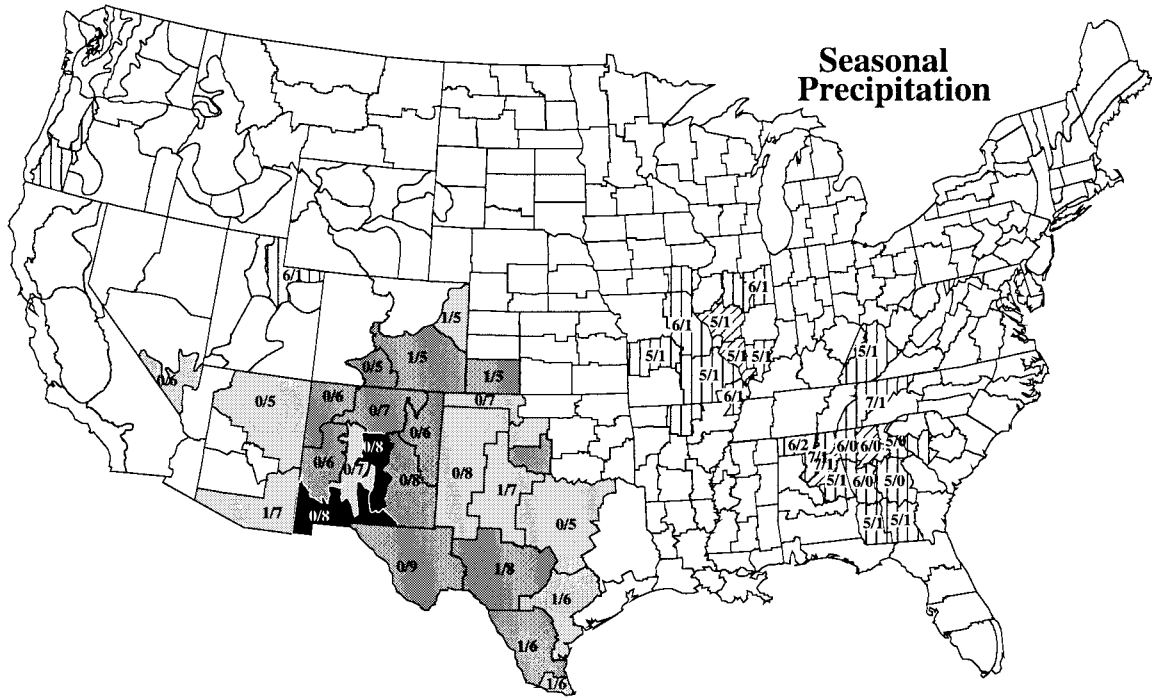


Shaded (hatched) climate divisions indicate areas that experienced a significant incidence of above (below) median seasonal climate. Confidence levels for skewness about the median can be found under the greyscale legend. Where climate divisions are annotated, a significant incidence of seasonal climate in the lowest or highest 25% of historical values was found, with (n/m) indicating n seasons in the lowest 25%, m seasons in the highest 25%.

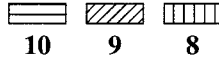
Figure A10: El Niño March-April-May

10 seasons

- 1900
- 1905
- 1914
- 1915
- 1919
- 1940
- 1941
- 1983
- 1987
- 1992



Below Median



10

9

8

Above Median

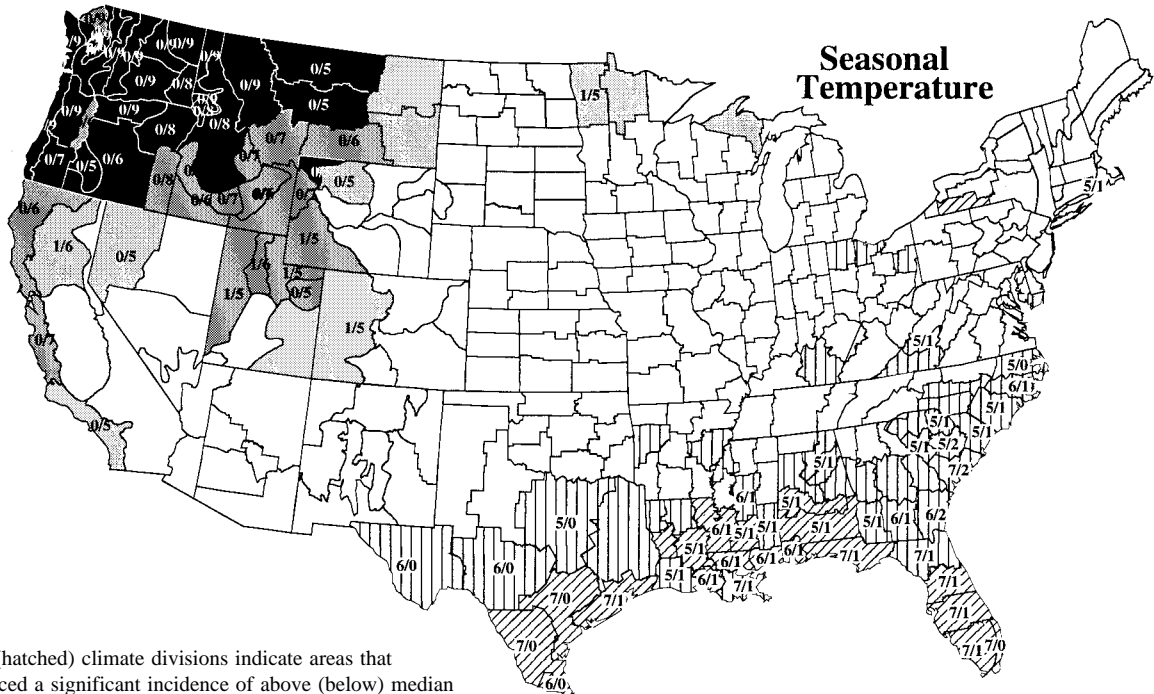


8

9

10

95.1% 99.1% 99.9%

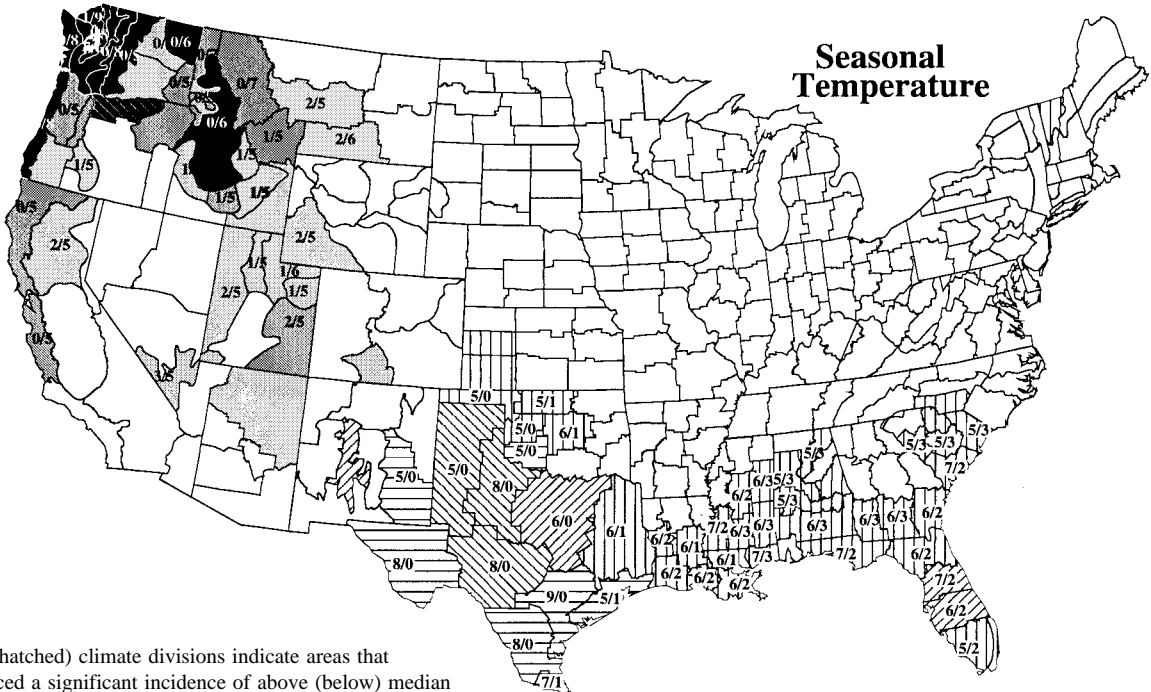
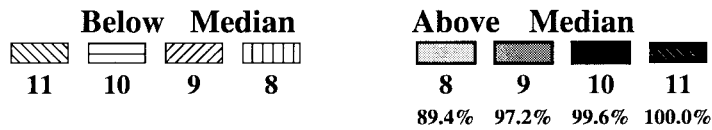
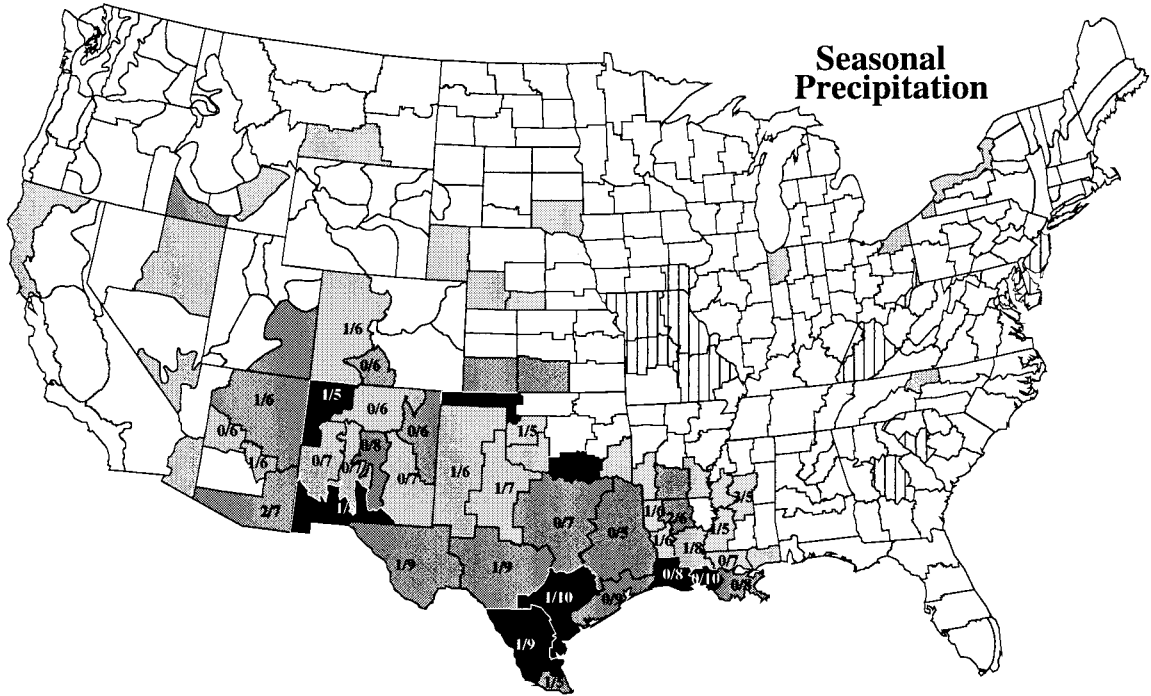


Shaded (hatched) climate divisions indicate areas that experienced a significant incidence of above (below) median seasonal climate. Confidence levels for skewness about the median can be found under the greyscale legend. Where climate divisions are annotated, a significant incidence of seasonal climate in the lowest or highest 25% of historical values was found, with (n/m) indicating n seasons in the lowest 25%, m seasons in the highest 25%.

Figure A11: El Niño April-May-June

11 seasons

- 1900
- 1905
- 1914
- 1919
- 1940
- 1941
- 1983
- 1987
- 1992
- 1993
- 1997



Shaded (hatched) climate divisions indicate areas that experienced a significant incidence of above (below) median seasonal climate. Confidence levels for skewness about the median can be found under the greyscale legend. Where climate divisions are annotated, a significant incidence of seasonal climate in the lowest or highest 25% of historical values was found, with (n/m) indicating n seasons in the lowest 25%, m seasons in the highest 25%.

APPENDIX B

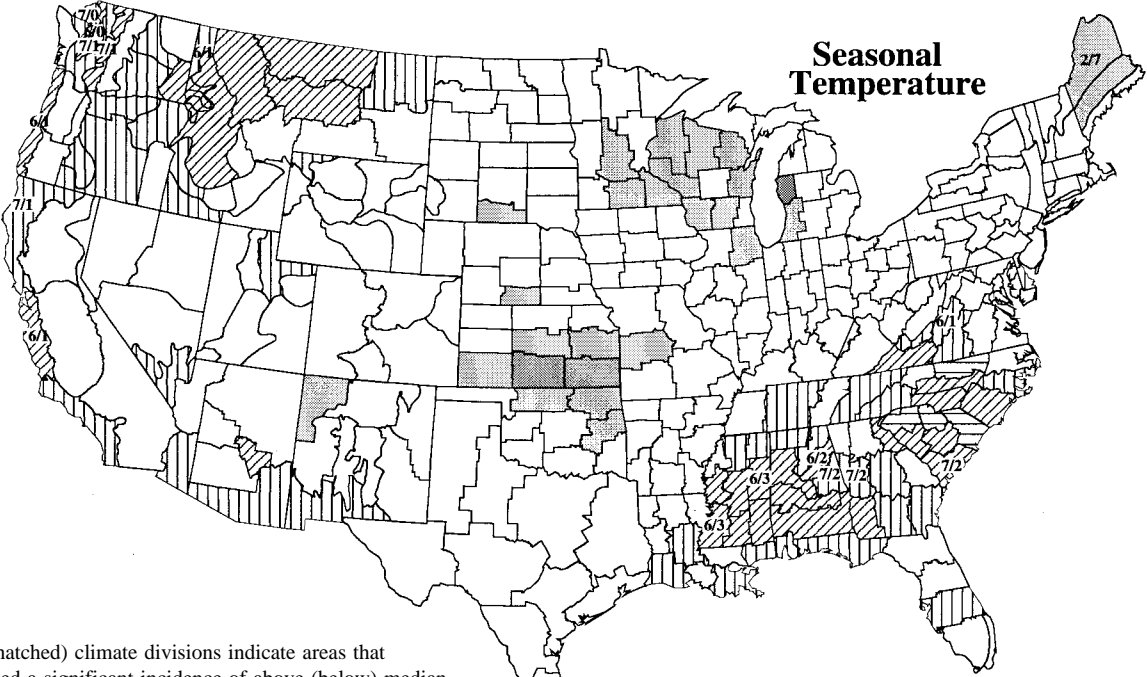
Figures B1-B10 show statistical analyses of cumulative rainfall (a) and mean temperature (b) for 3 month seasonal periods during which the average value of Wright's S index (Wright, 1989) was in the lowest 17% (< -0.64 C) of 1895-1997 values. The listed years refer to the years in which the first month of the 3 month periods fell, thus DJF 1908 refers to December-January-February of 1908/1909. As in Appendix A shaded (hatched) climate divisions indicate areas that experienced a significant incidence of above (below) median seasonal climate, and confidence levels for skewness about the median can be found under the greyscale legend. Where climate divisions are annotated, a significant incidence of seasonal climate in the lowest or highest 25% of historical values was found, with (n/m) indicating n seasons in the lowest 25%, m seasons in the highest 25%.

La Niña Precipitation and Temperature Analyses

Summer-Fall		Figure
	June-July-August (JJA)	B1
	July-August –September (JAS)	B2
	August –September-October (ASO)	B3
Fall-Winter		
	September-October-November (SON)	B4
	October-November-December (OND)	B5
	November-December-January (NDJ)	B6
	December-January –February (DJF)	B7
Winter-Spring		
	January –February –March (JFM)	B8
	February –March-April (FMA)	B9
	March-April-May (MAM)	B10
	April-May-June (AMJ)	B11

Figure B1: La Niña June-July-August

- 13 seasons
 1908
 1909
 1916
 1924
 1946
 1950
 1954
 1955
 1964
 1970
 1973
 1975
 1988

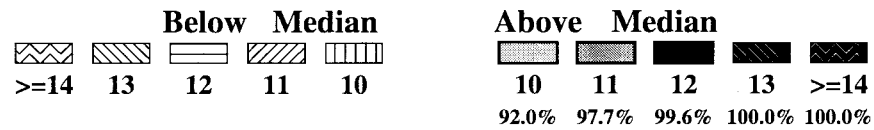


Shaded (hatched) climate divisions indicate areas that experienced a significant incidence of above (below) median seasonal climate. Confidence levels for skewness about the median can be found under the greyscale legend. Where climate divisions are annotated, a significant incidence of seasonal climate in the lowest or highest 25% of historical values was found, with (n/m) indicating n seasons in the lowest 25%, m seasons in the highest 25%.

Figure B2: La Niña July-August-September

14 seasons

- 1908
- 1909
- 1916
- 1924
- 1938
- 1942
- 1950
- 1954
- 1955
- 1964
- 1970
- 1973
- 1975
- 1988

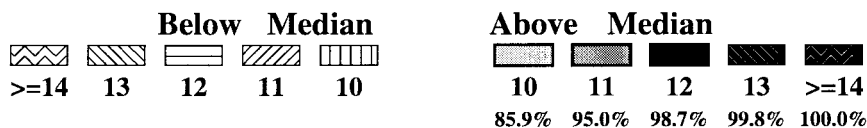


Shaded (hatched) climate divisions indicate areas that experienced a significant incidence of above (below) median seasonal climate. Confidence levels for skewness about the median can be found under the greyscale legend. Where climate divisions are annotated, a significant incidence of seasonal climate in the lowest or highest 25% of historical values was found, with (n/m) indicating n seasons in the lowest 25%, m seasons in the highest 25%.

Figure B3: La Niña August-September-October

15 seasons

- 1908
- 1909
- 1915
- 1916
- 1924
- 1933
- 1938
- 1942
- 1954
- 1955
- 1964
- 1970
- 1973
- 1975
- 1988

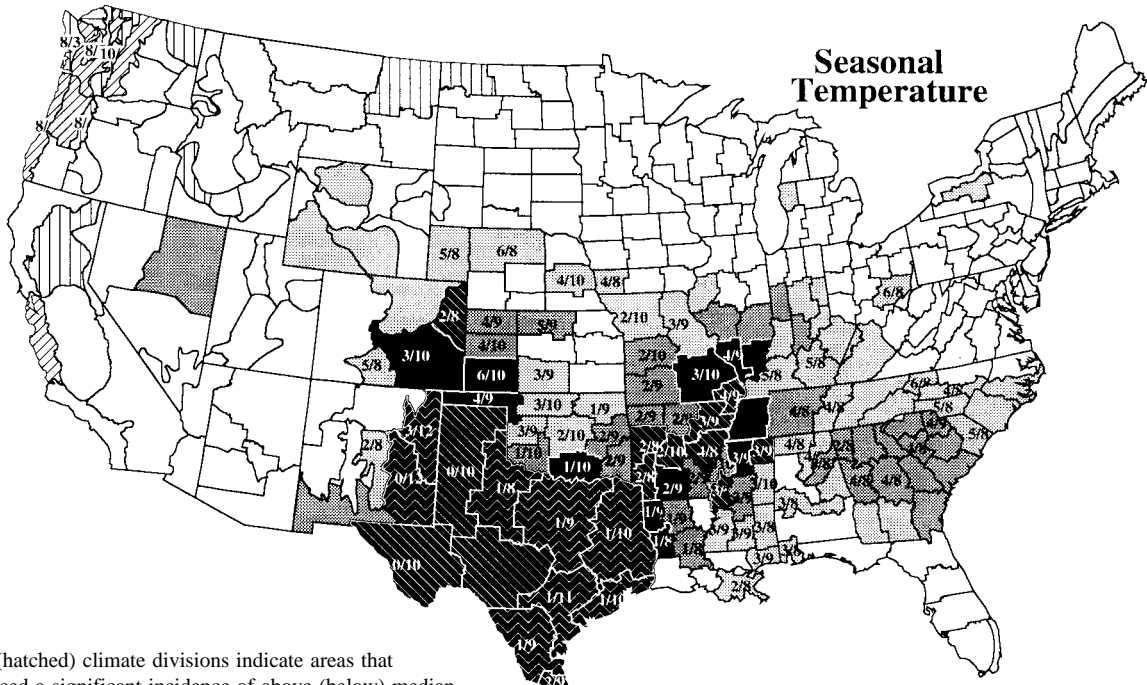
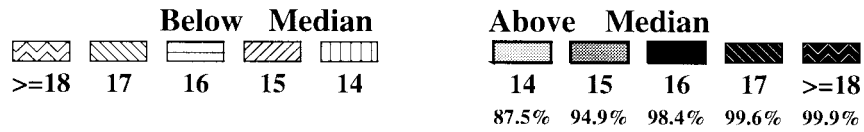
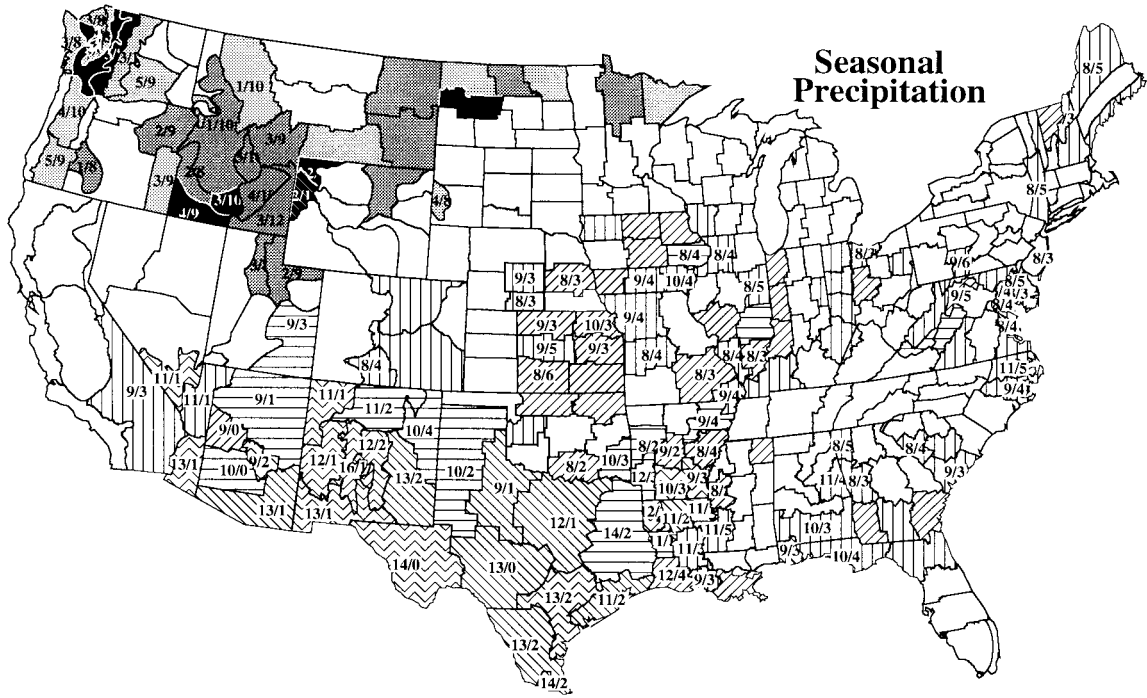


Shaded (hatched) climate divisions indicate areas that experienced a significant incidence of above (below) median seasonal climate. Confidence levels for skewness about the median can be found under the greyscale legend. Where climate divisions are annotated, a significant incidence of seasonal climate in the lowest or highest 25% of historical values was found, with (n/m) indicating n seasons in the lowest 25%, m seasons in the highest 25%.

Figure B5: La Niña October-November-December

22 seasons

- 1908
- 1909
- 1915
- 1916
- 1917
- 1922
- 1924
- 1933
- 1938
- 1942
- 1949
- 1950
- 1954
- 1955
- 1956
- 1964
- 1970
- 1971
- 1973
- 1975
- 1988
- 1995

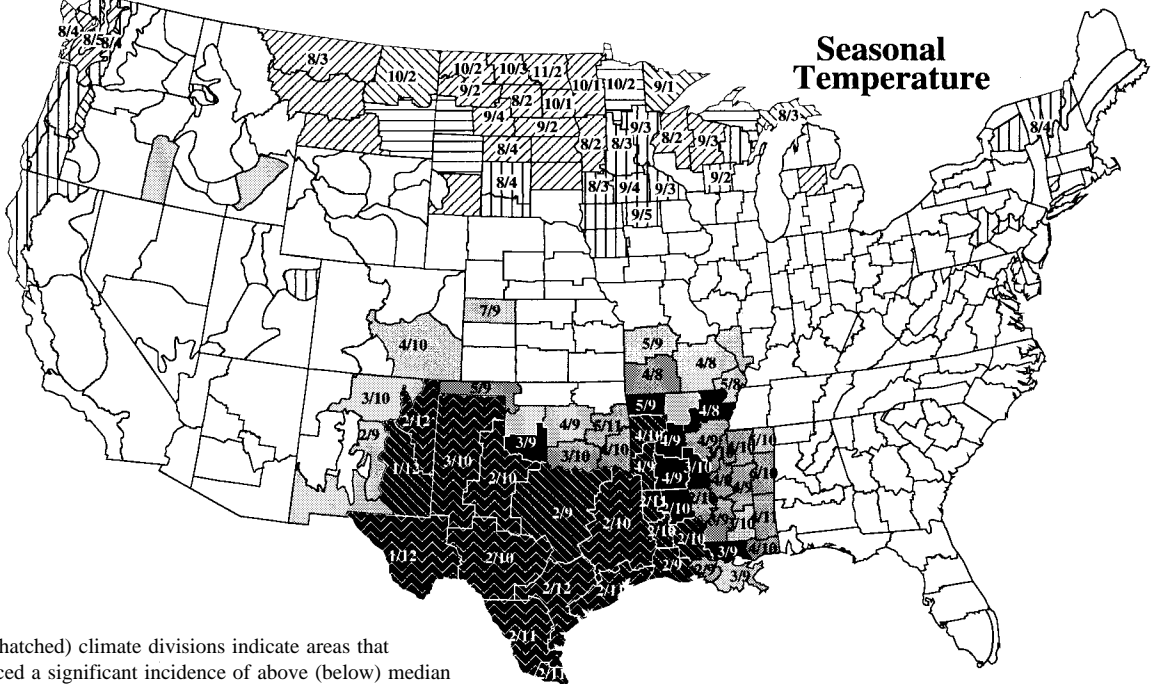
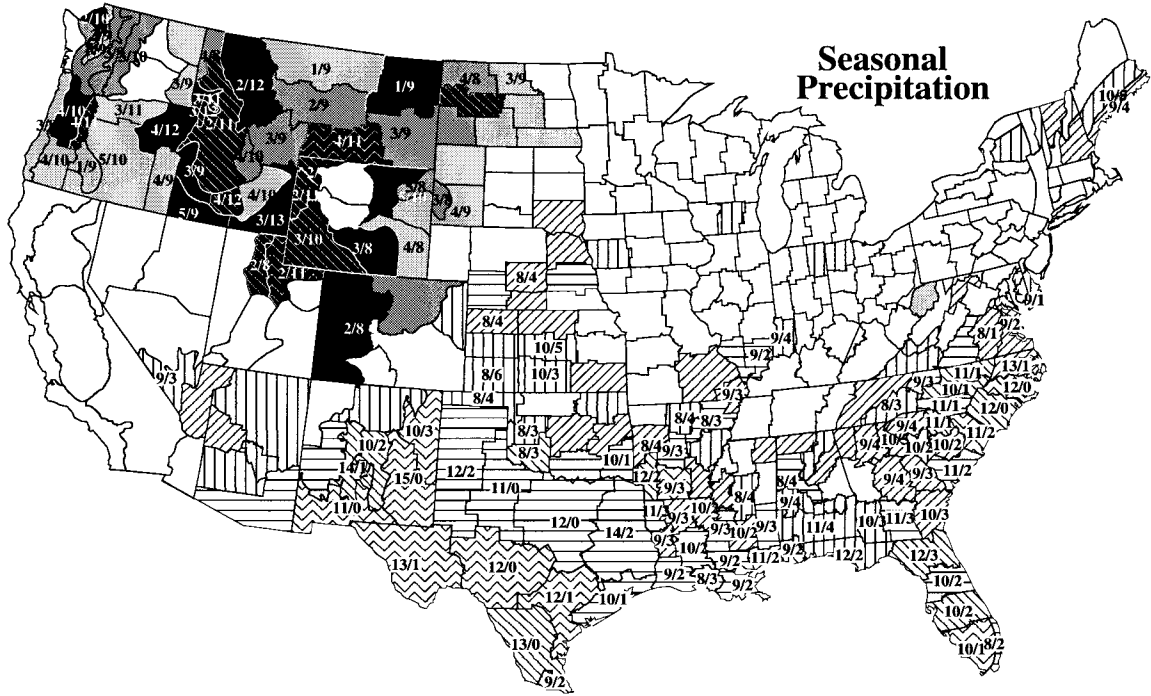


Shaded (hatched) climate divisions indicate areas that experienced a significant incidence of above (below) median seasonal climate. Confidence levels for skewness about the median can be found under the greyscale legend. Where climate divisions are annotated, a significant incidence of seasonal climate in the lowest or highest 25% of historical values was found, with (n/m) indicating n seasons in the lowest 25%, m seasons in the highest 25%.

Figure B6: La Niña November-December-January

22 seasons

- 1898
- 1908
- 1909
- 1910
- 1916
- 1917
- 1924
- 1933
- 1938
- 1942
- 1949
- 1950
- 1954
- 1955
- 1956
- 1964
- 1970
- 1971
- 1973
- 1975
- 1988
- 1995

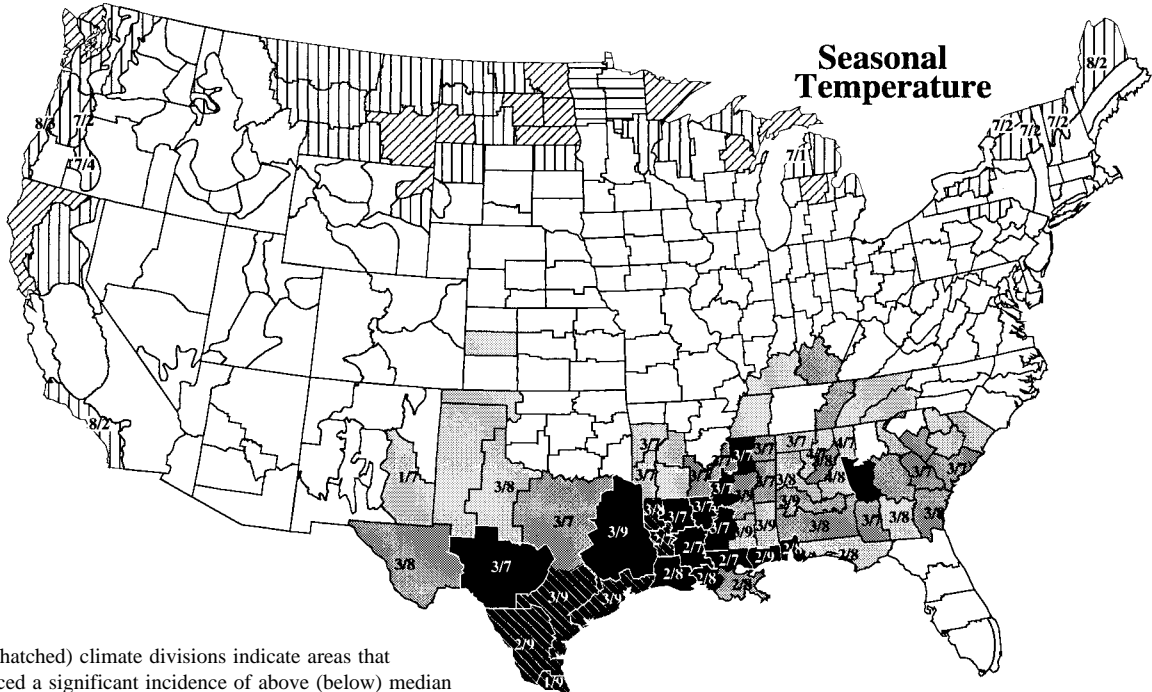
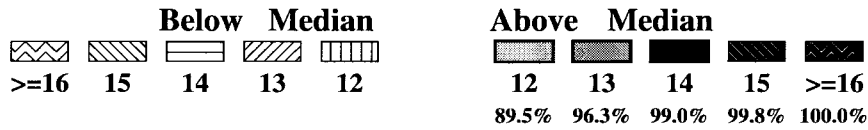
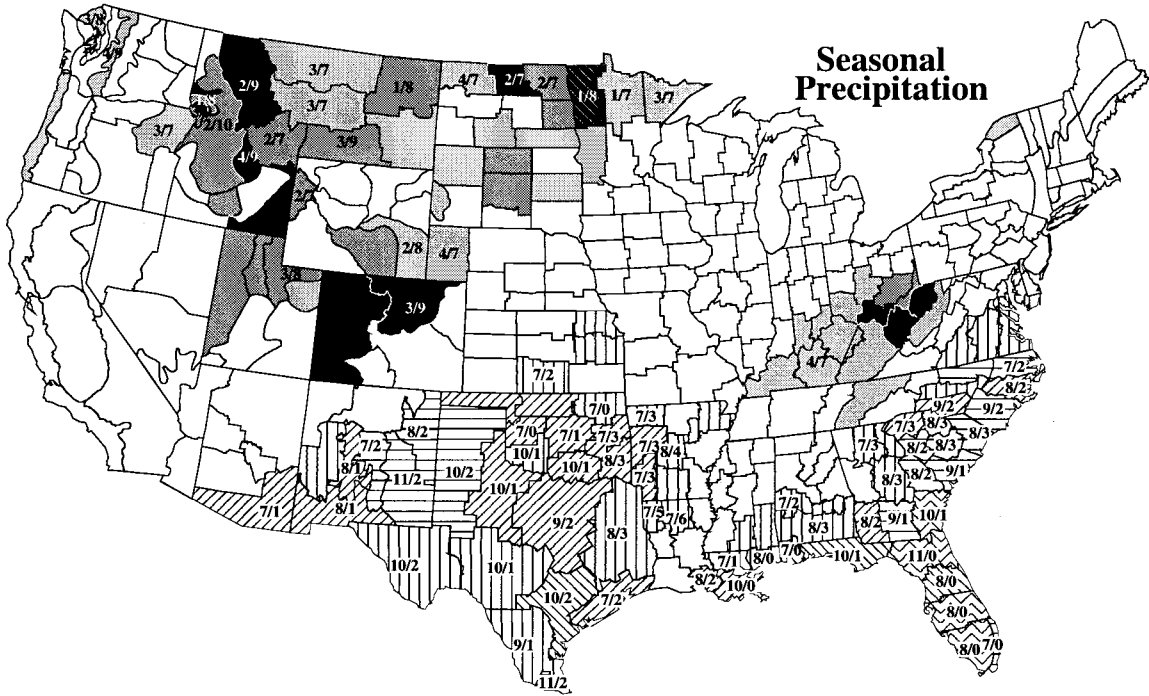


Shaded (hatched) climate divisions indicate areas that experienced a significant incidence of above (below) median seasonal climate. Confidence levels for skewness about the median can be found under the greyscale legend. Where climate divisions are annotated, a significant incidence of seasonal climate in the lowest or highest 25% of historical values was found, with (n/m) indicating n seasons in the lowest 25%, m seasons in the highest 25%.

Figure B7: La Niña December-January-February

18 seasons

- 1908
- 1909
- 1910
- 1916
- 1917
- 1924
- 1933
- 1938
- 1942
- 1949
- 1954
- 1955
- 1967
- 1970
- 1973
- 1975
- 1988
- 1995

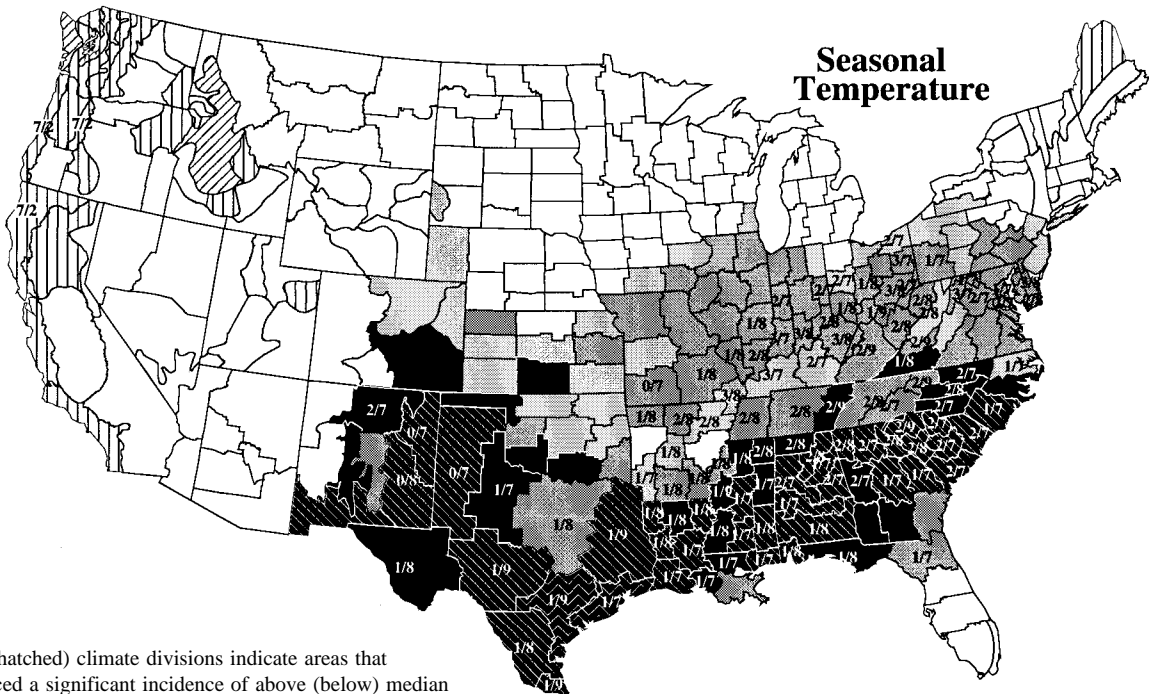
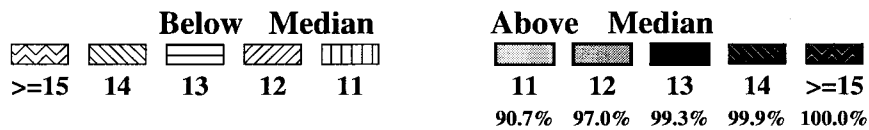
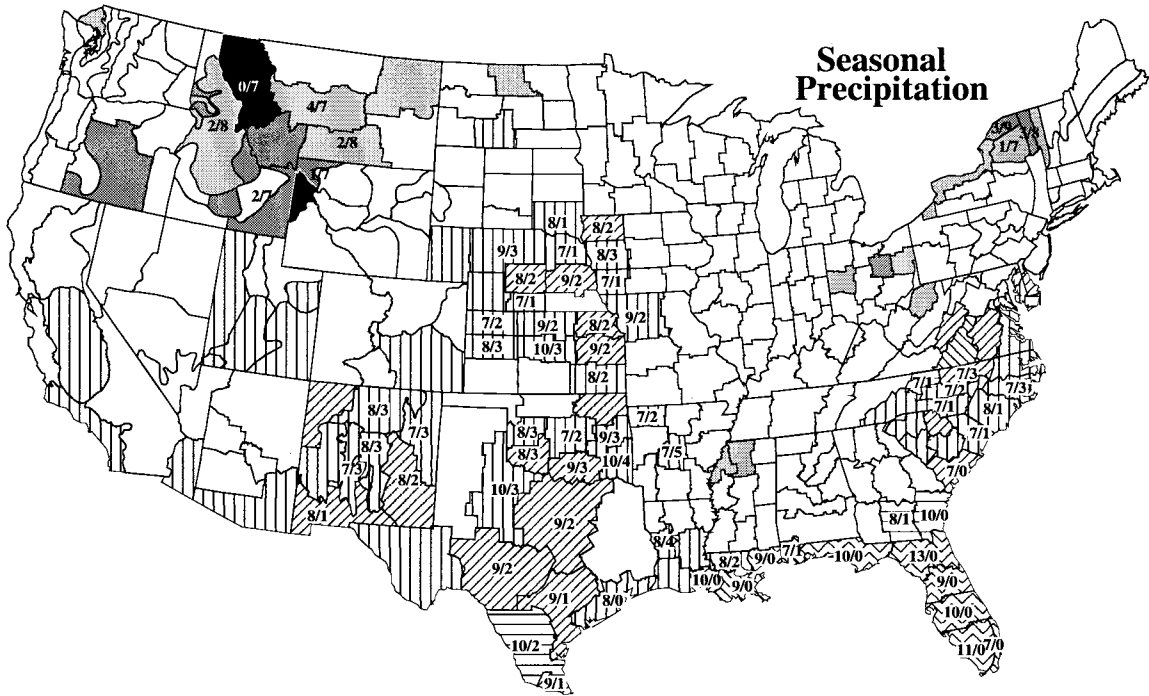


Shaded (hatched) climate divisions indicate areas that experienced a significant incidence of above (below) median seasonal climate. Confidence levels for skewness about the median can be found under the greyscale legend. Where climate divisions are annotated, a significant incidence of seasonal climate in the lowest or highest 25% of historical values was found, with (n/m) indicating n seasons in the lowest 25%, m seasons in the highest 25%.

Figure B8: La Niña January-February-March

18 seasons

- 1898
- 1909
- 1910
- 1911
- 1917
- 1918
- 1925
- 1939
- 1943
- 1950
- 1956
- 1968
- 1971
- 1974
- 1976
- 1989

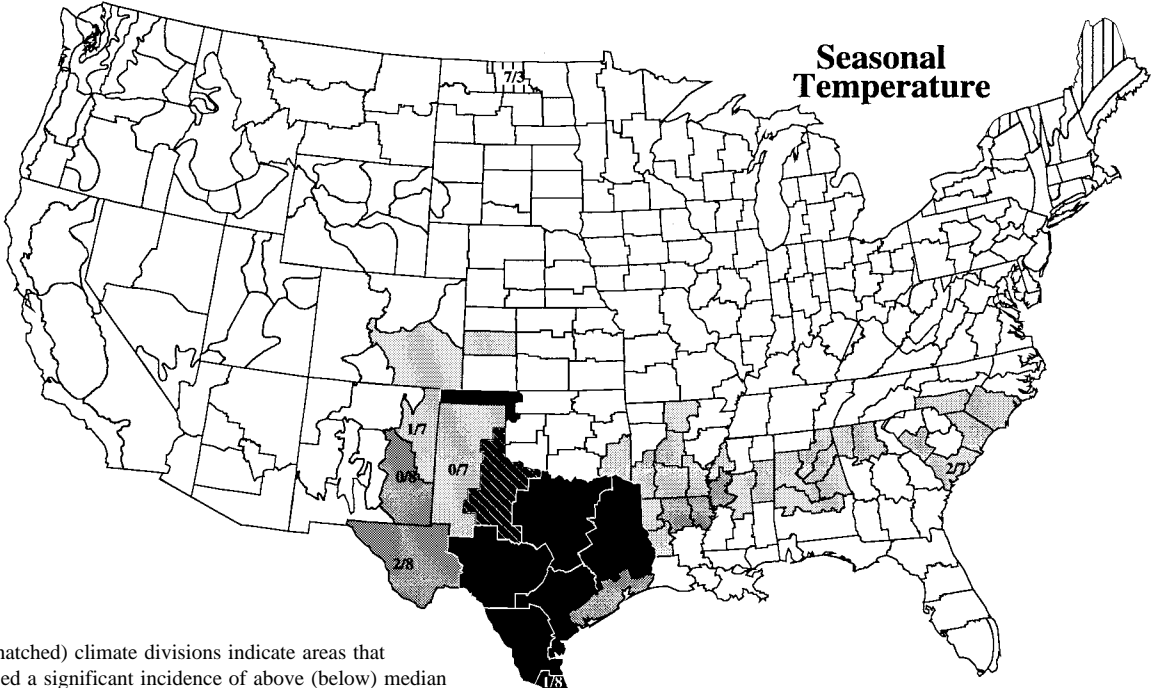
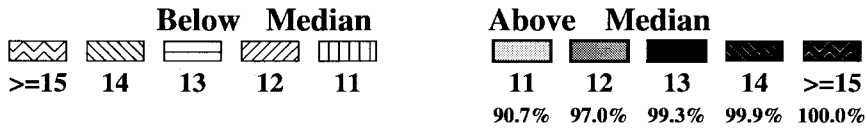
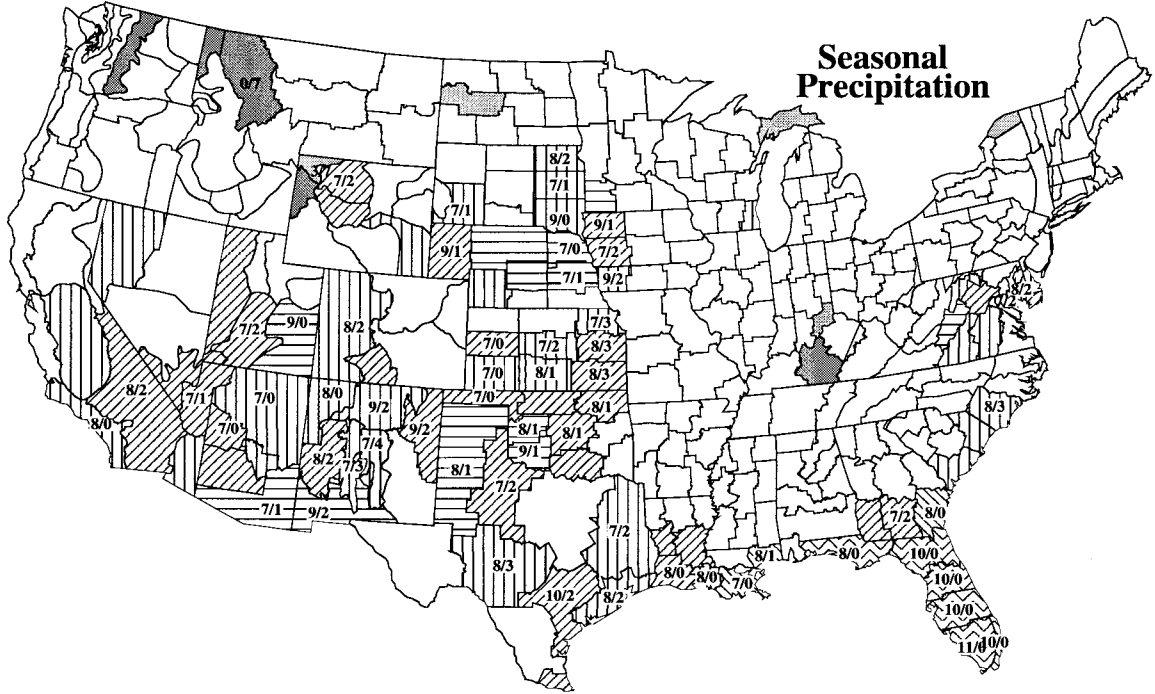


Shaded (hatched) climate divisions indicate areas that experienced a significant incidence of above (below) median seasonal climate. Confidence levels for skewness about the median can be found under the greyscale legend. Where climate divisions are annotated, a significant incidence of seasonal climate in the lowest or highest 25% of historical values was found, with (n/m) indicating n seasons in the lowest 25%, m seasons in the highest 25%.

Figure B9: La Niña February-March-April

16 seasons

- 1898
- 1909
- 1910
- 1911
- 1916
- 1917
- 1925
- 1939
- 1943
- 1945
- 1950
- 1956
- 1968
- 1971
- 1974
- 1989

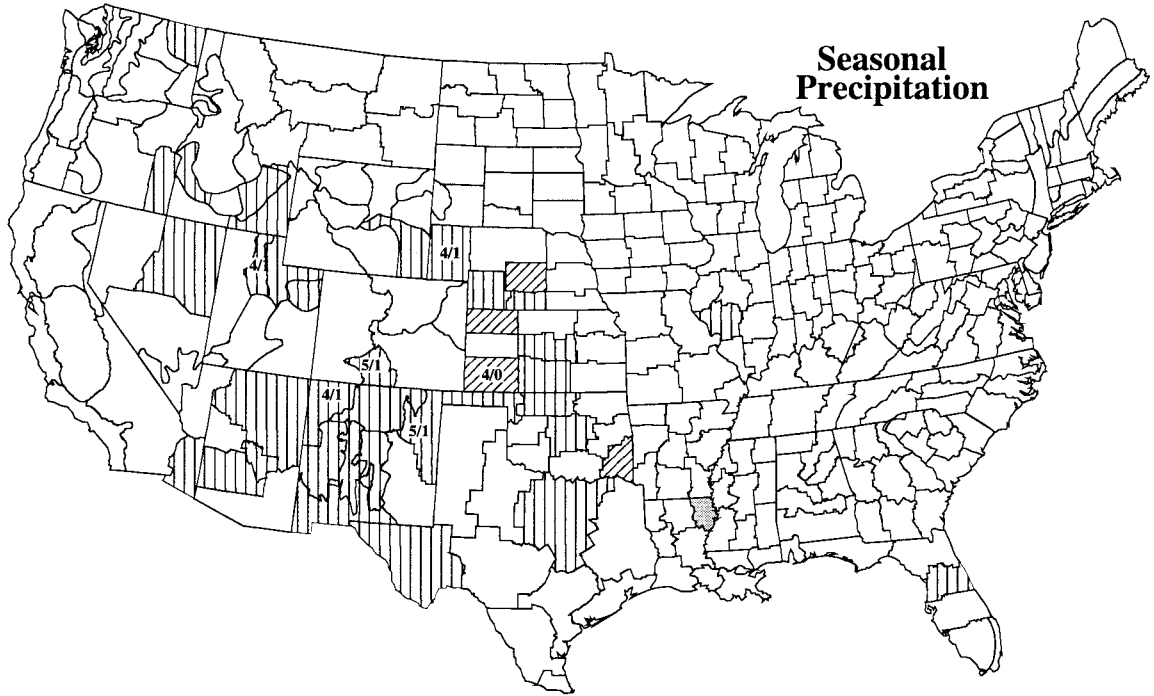


Shaded (hatched) climate divisions indicate areas that experienced a significant incidence of above (below) median seasonal climate. Confidence levels for skewness about the median can be found under the greyscale legend. Where climate divisions are annotated, a significant incidence of seasonal climate in the lowest or highest 25% of historical values was found, with (n/m) indicating n seasons in the lowest 25%, m seasons in the highest 25%.

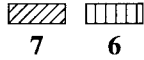
Figure B11: La Niña April-May-June

7 seasons

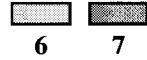
- 1909
- 1910
- 1916
- 1950
- 1954
- 1964
- 1988



Below Median



Above Median



94.1% 99.3%



Shaded (hatched) climate divisions indicate areas that experienced a significant incidence of above (below) median seasonal climate. Confidence levels for skewness about the median can be found under the greyscale legend. Where climate divisions are annotated, a significant incidence of seasonal climate in the lowest or highest 25% of historical values was found, with (n/m) indicating n seasons in the lowest 25%, m seasons in the highest 25%.

APPENDIX C

Figures C1-C3 show statistical analyses of cumulative rainfall (a) and mean temperature (b) for JJA, JAS, and ASO Summer-Fall seasonal periods during which the average value of Wright's S index (Wright, 1989) was in the lowest 10% (< -0.84 C) of 1895-1997 values. As in Appendix A and B, shaded (hatched) climate divisions indicate areas that experienced a significant incidence of above (below) median seasonal climate, and confidence levels for skewness can be found under the greyscale legend. Where climate divisions are annotated, a significant incidence of seasonal climate in the lowest or highest 25% of historical values was found, with (n/m) indicating n seasons in the lowest 25%, m seasons in the highest 25%.

La Niña Precipitation and Temperature Analyses

Summer-Fall

	Figure
June-July-August (JJA)	C1
July-August –September (JAS)	C2
August –September-October (ASO)	C3

Figure C1: La Niña June-July-August

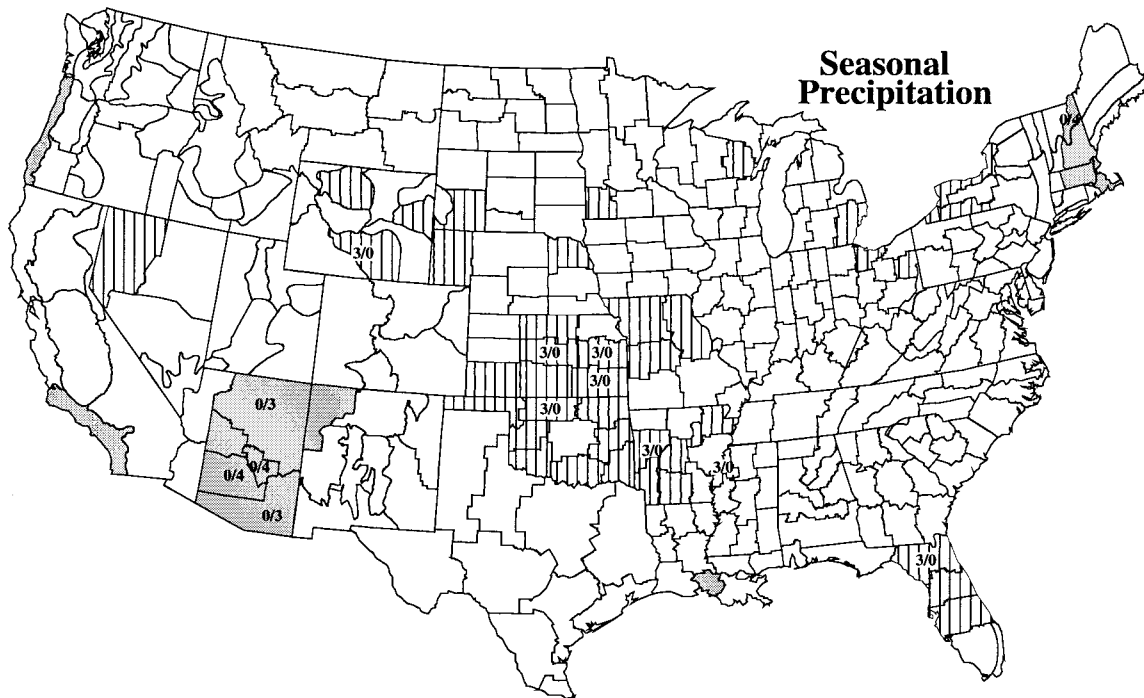
4 seasons

1916

1954

1955

1988



Below Median



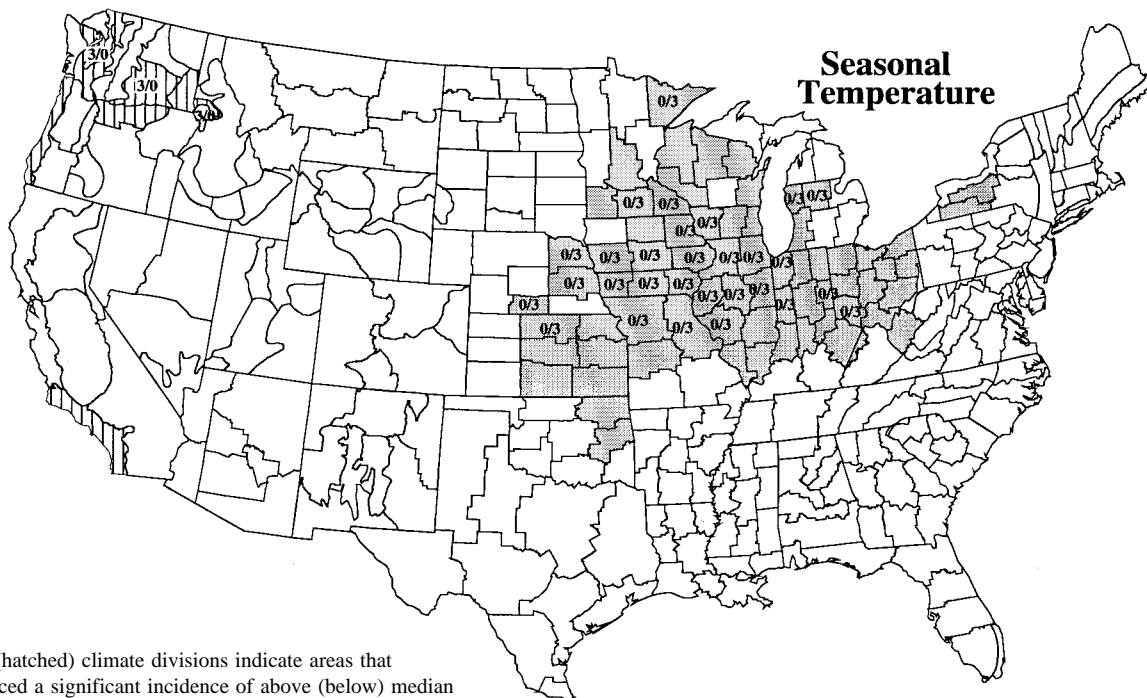
4

Above Median



4

93.9%

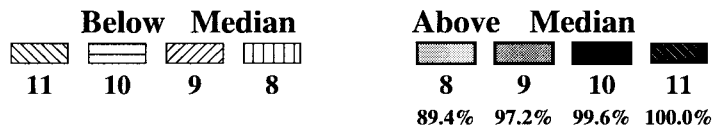


Shaded (hatched) climate divisions indicate areas that experienced a significant incidence of above (below) median seasonal climate. Confidence levels for skewness about the median can be found under the greyscale legend. Where climate divisions are annotated, a significant incidence of seasonal climate in the lowest or highest 25% of historical values was found, with (n/m) indicating n seasons in the lowest 25%, m seasons in the highest 25%.

Figure C3: La Niña August-September-October

11 seasons

- 1909
- 1915
- 1916
- 1938
- 1942
- 1954
- 1955
- 1970
- 1973
- 1975
- 1988



Shaded (hatched) climate divisions indicate areas that experienced a significant incidence of above (below) median seasonal climate. Confidence levels for skewness about the median can be found under the greyscale legend. Where climate divisions are annotated, a significant incidence of seasonal climate in the lowest or highest 25% of historical values was found, with (n/m) indicating n seasons in the lowest 25%, m seasons in the highest 25%.